Final Report

Alkali Silica Reaction (ASR) in Cement Free Alkali Activated Sustainable Concrete

Performing Organization: Clarkson University

December 2016

University Transportation Research Center - Region 2

The Region 2 University Transportation Research Center (UTRC) is one of ten original University Transportation Centers established in 1987 by the U.S. Congress. These Centers were established with the recognition that transportation plays a key role in the nation's economy and the quality of life of its citizens. University faculty members provide a critical link in resolving our national and regional transportation problems while training the professionals who address our transportation systems and their customers on a daily basis.

The UTRC was established in order to support research, education and the transfer of technology in the field of transportation. The theme of the Center is "Planning and Managing Regional Transportation Systems in a Changing World." Presently, under the direction of Dr. Camille Kamga, the UTRC represents USDOT Region II, including New York, New Jersey, Puerto Rico and the U.S. Virgin Islands. Functioning as a consortium of twelve major Universities throughout the region, UTRC is located at the CUNY Institute for Transportation Systems at The City College of New York, the lead institution of the consortium. The Center, through its consortium, an Agency-Industry Council and its Director and Staff, supports research, education, and technology transfer under its theme. UTRC's three main goals are:

Research

The research program objectives are (1) to develop a theme based transportation research program that is responsive to the needs of regional transportation organizations and stakeholders, and (2) to conduct that program in cooperation with the partners. The program includes both studies that are identified with research partners of projects targeted to the theme, and targeted, short-term projects. The program develops competitive proposals, which are evaluated to insure the mostresponsive UTRC team conducts the work. The research program is responsive to the UTRC theme: "Planning and Managing Regional Transportation Systems in a Changing World." The complex transportation system of transit and infrastructure, and the rapidly changing environment impacts the nation's largest city and metropolitan area. The New York/New Jersey Metropolitan has over 19 million people, 600,000 businesses and 9 million workers. The Region's intermodal and multimodal systems must serve all customers and stakeholders within the region and globally.Under the current grant, the new research projects and the ongoing research projects concentrate the program efforts on the categories of Transportation Systems Performance and Information Infrastructure to provide needed services to the New Jersey Department of Transportation, New York City Department of Transportation, New York Metropolitan Transportation Council , New York State Department of Transportation, and the New York State Energy and Research Development Authorityand others, all while enhancing the center's theme.

Education and Workforce Development

The modern professional must combine the technical skills of engineering and planning with knowledge of economics, environmental science, management, finance, and law as well as negotiation skills, psychology and sociology. And, she/he must be computer literate, wired to the web, and knowledgeable about advances in information technology. UTRC's education and training efforts provide a multidisciplinary program of course work and experiential learning to train students and provide advanced training or retraining of practitioners to plan and manage regional transportation systems. UTRC must meet the need to educate the undergraduate and graduate student with a foundation of transportation fundamentals that allows for solving complex problems in a world much more dynamic than even a decade ago. Simultaneously, the demand for continuing education is growing – either because of professional license requirements or because the workplace demands it – and provides the opportunity to combine State of Practice education with tailored ways of delivering content.

Technology Transfer

UTRC's Technology Transfer Program goes beyond what might be considered "traditional" technology transfer activities. Its main objectives are (1) to increase the awareness and level of information concerning transportation issues facing Region 2; (2) to improve the knowledge base and approach to problem solving of the region's transportation workforce, from those operating the systems to those at the most senior level of managing the system; and by doing so, to improve the overall professional capability of the transportation workforce; (3) to stimulate discussion and debate concerning the integration of new technologies into our culture, our work and our transportation systems; (4) to provide the more traditional but extremely important job of disseminating research and project reports, studies, analysis and use of tools to the education, research and practicing community both nationally and internationally; and (5) to provide unbiased information and testimony to decision-makers concerning regional transportation issues consistent with the UTRC theme.

Principal Investigator(s):
Sulapha Peethamparan
Associate Professor
Department of Civil & Environmental Engineering
Clarkson University
Potsdam, NY 13699
Phone: (315)-268-4435
Email: speetham@clarkson.edu

To request a hard copy of our final reports, please send us an email at utrc@utrc2.org

Mailing Address:

University Transportation Reserch Center
The City College of New York
Marshak Hall, Suite 910
160 Convent Avenue
New York, NY 10031
Tel: 212-650-8051
Fax: 212-650-8374
Web: www.utrc2.org

Board of Directors

The UTRC Board of Directors consists of one or two members from each Consortium school (each school receives two votes regardless of the number of representatives on the board). The Center Director is an ex-officio member of the Board and The Center management team serves as staff to the Board.

City University of New York
Dr. Hongmian Gong - Geography/Hunter College
Dr. Neville A. Parker - Civil Engineering/CCNY

Clarkson University
Dr. Kerop D. Janoyan - Civil Engineering

Columbia University
Dr. Raimondo Betti - Civil Engineering
Dr. Elliott Sclar - Urban and Regional Planning

Cornell University
Dr. Huaizhu (Oliver) Gao - Civil Engineering

Hofstra University
Dr. Jean-Paul Rodrigue - Global Studies and Geography

Manhattan College
Dr. Anirban De - Civil & Environmental Engineering
Dr. Matthew Volovski - Civil & Environmental Engineering

New Jersey Institute of Technology
Dr. Steven I-Jy Chien - Civil Engineering
Dr. Joyoung Lee - Civil & Environmental Engineering

New York University
Dr. Mitchell L. Moss - Urban Policy and Planning
Dr. Rae Zimmerman - Planning and Public Administration

Polytechnic Institute of NYU
Dr. Kaan Ozbay - Civil Engineering
Dr. John C. Falcocchio - Civil Engineering
Dr. Elena Prassas - Civil Engineering

Rensselaer Polytechnic Institute
Dr. José Holguín-Veras - Civil Engineering
Dr. William "Al" Wallace - Systems Engineering

Rochester Institute of Technology
Dr. James Winebrake - Science, Technology and Society/Public Policy
Dr. J. Scott Hawker - Software Engineering

Rowan University
Dr. Yusuf Mehta - Civil Engineering
Dr. Beena Sukumaran - Civil Engineering

State University of New York
Michael M. Fancher - Nanoscience
Dr. Catherine T. Lawson - City & Regional Planning
Dr. Adel W. Sadek - Transportation Systems Engineering
Dr. Shmuel Yahalom - Economics

Stevens Institute of Technology
Dr. Sophia Hassiotis - Civil Engineering
Dr. Thomas H. Wakeman III - Civil Engineering

Syracuse University
Dr. Riyad S. Aboutaha - Civil Engineering
Dr. O. Sam Salem - Construction Engineering and Management

The College of New Jersey
Dr. Thomas M. Brennan Jr - Civil Engineering

University of Puerto Rico - Mayagüez
Dr. Ismael Pagán-Trinidad - Civil Engineering
Dr. Didier M. Valdés-Díaz - Civil Engineering

UTRC Consortium Universities

The following universities/colleges are members of the UTRC consortium.

City University of New York (CUNY)
Clarkson University (Clarkson)
Columbia University (Columbia)
Cornell University (Cornell)
Hofstra University (Hofstra)
Manhattan College (MC)
New Jersey Institute of Technology (NJIT)
New York Institute of Technology (NYIT)
New York University (NYU)
Rensselaer Polytechnic Institute (RPI)
Rochester Institute of Technology (RIT)
Rowan University (Rowan)
State University of New York (SUNY)
Stevens Institute of Technology (Stevens)
Syracuse University (SU)
The College of New Jersey (TCNJ)
University of Puerto Rico - Mayagüez (UPRM)

UTRC Key Staff

Dr. Camille Kamga: *Director, Assistant Professor of Civil Engineering*

Dr. Robert E. Paaswell: *Director Emeritus of UTRC and Distinguished Professor of Civil Engineering, The City College of New York*

Herbert Levinson: *UTRC Icon Mentor, Transportation Consultant and Professor Emeritus of Transportation*

Dr. Ellen Thorson: *Senior Research Fellow, University Transportation Research Center*

Penny Eickemeyer: *Associate Director for Research, UTRC*

Dr. Alison Conway: *Associate Director for Education*

Nadia Aslam: *Assistant Director for Technology Transfer*

Nathalie Martinez: *Research Associate/Budget Analyst*

Tierra Fisher*: Office Assistant*

Bahman Moghimi*: Research Assistant; Ph.D. Student, Transportation Program*

Wei Hao*: Research Fellow*

Andriy Blagay: *Graphic Intern*

1. Report No.	2.Government Accession No.	3. Recipient's Catalog No.

4. Title and Subtitle	5. Report Date
Alkali Silica Reaction (ASR) in Cement Free Alkali Activated Sustainable Concrete	12/19/16
	6. Performing Organization Code

7. Author(s)	8. Performing Organization Report No.
Zihui Li, Robert J. Thomas, Diego Lazama, Sulapha Peethamparon	

9. Performing Organization Name and Address	10. Work Unit No.
Clarkson University	
	11. Contract or Grant No.
	49198-35-27

12. Sponsoring Agency Name and Address	13. Type of Report and Period Covered
UTRC, The City College of New York 137th Street and Convent Ave. New York, NY 10031	final, May 30, 2015-December 31, 2016
	14. Sponsoring Agency Code

15. Supplementary Notes

16. Abstract

This report summarizes the findings of an experimental evaluation into alkali silica reaction (ASR) in cement free alkali-activated slag and fly ash binder concrete. The susceptibility of alkali-activated fly ash and slag concrete binders to deleterious ASR was evaluated in accordance with relevant ASTM standards. Also, ASR resistance of Alkali activated fly ash and slag concrete was compared to that of ordinary portland cement concrete (OPC) while exposed to ASTM C 1293 and ASTM C1567 tests. Special attention was given to assess the effectiveness of existing ASTM test methods (ASTM C 1293 and C1567) in identifying the occurrence of ASR in AAC. Additionally, influence of activator parameters including effect of binder type, activator concentration, activator type and solution to bonder ratio to the resistance of ASR in AAC was also evaluated. Finally, scanning electron microscopy (SEM) coupled with Energy Dispersive X-ray (EDX) analyses were used to confirm or repudiate the ASTM standard test results.

17. Key Words	18. Distribution Statement
alkali silica reaction	

19. Security Classif (of this report)	20. Security Classif. (of this page)	21. No of Pages	22. Price
Unclassified	Unclassified	61	

Form DOT F 1700.7 (8-69)

Disclaimer

The contents or conclusions from this report do not necessarily reflect the official view of the University Transport Center (UTRC) or the Federal Highway Administration. The contents of this report reflects the views of the authors, who are responsible for the facts and accuracy of the information herein. This report does not constitute a standard, specification, or regulation. This document is disseminated under the financial support of the Department of Transportation, University Transportation Center Program, in the interest of information exchange. The U.S. Government assumes no liability for the contents or use thereof.

Summary

This report summarizes the findings of an experimental evaluation into alkali silica reaction (ASR) in cement free alkali-activated slag and fly ash binder concrete. The susceptibility of alkali-activated fly ash and slag concrete binders to deleterious ASR was evaluated in accordance with relevant ASTM standards. Also, ASR resistance of Alkali activated fly ash and slag concrete was compared to that of ordinary portland cement concrete (OPC) while exposed to ASTM C 1293 and ASTM C1567 tests. Special attention was given to assess the effectiveness of existing ASTM test methods (ASTM C 1293 and C1567) in identifying the occurrence of ASR in AAC. Additionally, influence of activator parameters including effect of binder type, activator concentration, activator type and solution to bonder ratio to the resistance of ASR in AAC was also evaluated. Finally, scanning electron microscopy (SEM) coupled with Energy Dispersive X-ray (EDX) analyses were used to confirm or repudiate the ASTM standard test results.

The expansion of all the concrete mixtures made with alkali activated slag binders and non-reactive aggregate was within the stipulated 1000 $\mu\varepsilon$ limit under the ASTM C1567 test method. As per the standard, none of those mixtures was likely to cause any ASR reaction. Nevertheless, some of those same mixtures evaluated under ASTM C 1293 exhibited expansion strains beyond 400 $\mu\varepsilon$ stipulated by ASTM C1293 at the end of one year exposure time. Extensive petrographic analyses of those samples using SEM and EDX could not identify ASR gel formation or cracking of aggregate in any of those mixtures and thus repudiating the ASTM C 1293 test results. All the samples that showed an expansion beyond the limit stipulated by the ASTM C1293 also had higher autogenous shrinkages during the initial hydration period. The internal humidity of those samples were also significantly low before exposing them to ASTM C 1293 test conditions. It appears that these samples absorbed more water and expanded because of

exposing them to 100% RH as per ASTM C1293. Additionally, most of those expansion strains occurred during the initial period of exposure to ASTM C 1293 test conditions. Thus, these expansions do not indicate the occurrence of ASR. Hence additional care should be taken to evaluate ASR resistance of concrete mixtures with high autogenous shrinkages (and low internal RH) using ASTM C1293 to avoid false positive results. Both the test methods and the petrography analyses confirmed the occurrence of ASR reaction in alkali activated slag concrete with reactive aggregate.

For alkali activated fly ash concretes, both C1293 and C1567 (except one or two cases) results were consistent with no expansion beyond the stipulated limit of each of the codes. The SEM and EDX analysis also supported the findings, no ASR gel was detected in concrete with none reactive aggregates. Concrete with reactive aggregate expanded beyond the limits of the codes and extensive cracking was found in the reactive aggregate containing concrete during the SEM analysis.

In summary, no deleterious ASR occurred in AAC concrete unless highly reactive aggregate was used in the mixture. Additionally, ASR reaction product (ASR gel) was found only in AAC concrete with reactive aggregate. The morphology and chemical composition was similar to that typically found in OPC concrete system. The mixture parameters, including silica modulus, sodium oxide percentage, activator type and solution to binder ratio, have some extent of influence on the mass change and expansion of the specimens. However, there was no evidence to show that these parameters can significantly affect the alkali-silica reactivity in AAC. It can be suggested from this study that both long-term ASTM test method C1293 and ASTM test method C1567 are effective in detecting the occurrence of alkali-silica reaction in AAC concrete but care should be taken to interpret the results.

Figure list

Table list

1.Introduction

1.1 Motivation

Portland cement concrete is the most widely used construction material in the world. However, the manufacture of ordinary portland cement (OPC) is highly energy-intensive and produces a significant quantity of greenhouse gas emissions. Portland cement manufacture involves mining, grinding, blending of raw materials, clinkering in a rotary kiln above 1450 ℃, milling, packing, and transportation of the final products. The manufacture and transportation of a single ton of portland cement consumes 3.2-5.8 GJ and results in the emission of 0.95 ton of CO_2. The manufacture of portland cement is responsible for up to 7% of global anthropogenic carbon emissions[1-3]. Increasing awareness of the societal and environmental impact of portland cement manufacture has inspired an industry-wide effort to develop sustainable alternative binders for concrete.

Alkali-activated concrete (AAC), made by the activation of fly ashes or slag cement with strong alkalis, is rapidly emerging as a promising sustainable alternative to portland cement concrete. In recent decades, the hydration mechanism, mechanic properties, reaction productions and durability of AAC has been extensively studied[4-8]. Additional to the environment benefits of reduced carbon emission and energy consumption [9, 10], these alternative binder materials are known to improve the mechanical properties and durability while been exposed to different environments [7, 11-14].

Despite the improved performance and sustainability of AAC, its application as viable construction materials has not been realized. This is mainly due to the result of several remaining technical barriers, one of them is the uncertainty with respect to the alkali-silica reactivity of

AAC. It was suggested that alkali-activated binder concretes might be more vulnerable to alkali-silica reaction (ASR) than OPC, because of the high alkalinity of the activator. On the other hand, alkali-activated binders are devoid of the Ca^{2+} that play a vital role in the formation of ASR gel in OPC, and may therefore be immune to any associated problems. Several investigations have been undertaken by researchers to verify the occurrence of ASR in AAC system *(15)*. Nevertheless, several questions remain unanswered. The objective of this research is to increase the knowledge in the existing literature on the occurrence of ASR in alkali activated binder concrete systems.

1.2 Alkali-silica-reaction (ASR) in ordinary Portland cement (OPC) concrete

Alkali-silica-reaction (ASR), can defined as a deleterious reaction, which occurs over time in concrete between high alkali pore fluid and the reactive non-crystalline (amorphous) silica in aggregates particles. In general, the aggregates that cause harmful reactions in concrete are those containing amorphous silica (silicate glasses and opal), unstable crystalline polymorphs of silica (cristobalite and tridymite), poorly crystalline forms of silica, and microcrystalline quartz-bearing rocks. During this chemical reaction, moisture (water) is required in order to form the alkali-silica gel, and the gel swells which cause degradation of concrete with the absorption of moisture. The expansion the reaction product will generate pressure within concrete and result in various forms of deterioration in the concrete including cracking, expansion, and "pops-out"*(16)*. The typical microstructure image of deleterious ASR occurred in OPC concrete is shown in Fig.1.
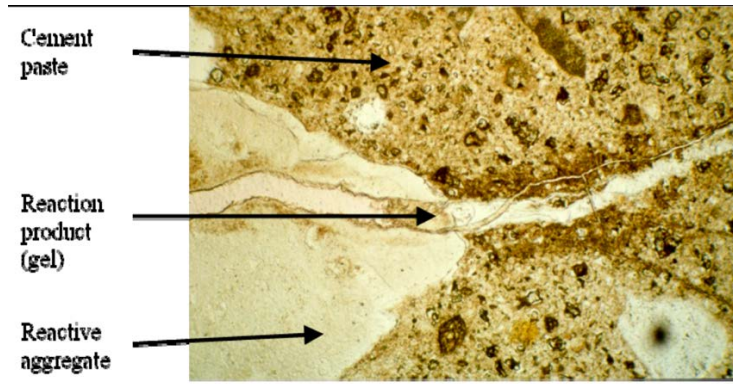
Fig.1 The scanning electron microscopy (SEM) image of ASR in OPC concrete*(17)*

The alkali-silica reaction can be idealized as the following reaction:

$$4 \, Si_2O + 2 \, NaOH = Na_2Si_4O_9 + H_2O$$

$$Si_2O + 2NaOH = Na_2O_3 + H_2O$$
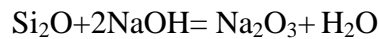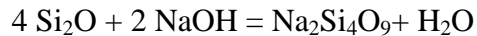
Alkali silica reaction in OPC concrete was extensively investigated by researchers and scientists in last several decades, and its mechanism and typical cause were well documented in the literature*(16, 18)*. It is clear that three factors were required for a damaging alkali silica reaction to occur; These are:

1) A sufficient quantity of reactive silica in aggregate;

2) Enough concentration of alkali (hydroxyl group);

3) Sufficient amount of moisture;

Some evidence shows that calcium must be available for damaging ASR to occur, although the exact role of calcium in this process has not been identified. Thus, reducing the availability of calcium in the concrete system, such as blended pozzolanic supplementary materials in the mixture, has been employed as a way to to prevent the occurrence of ASR*(16)*.

1.3 Alkali-silica-reaction (ASR) in alkali-activated concrete (AAC)

The ASR mechanism and mitigation of ASR within portland cement binders was generally well-understood. However, comparatively little is known about ASR in alkali-activated fly ash and slag binder concretes. A number of researchers have investigated the occurrence of ASR in AAC system, but no consensus conclusions can be draw from the existing literature. Davidovits reported shrinkage in alkali activated mortars subjected to the ASTM C227 mortar bar test method, while OPC mortars under the same conditions expanded significantly *(19)*. Jimenez suggested that some expansion could occur in alkali activated binders exposed to these test methods, but would be much smaller in magnitude than that in OPC binders *(20)*. Puertas confirmed that ASR could occur in alkali activated slag concrete containing reactive siliceous aggregate *(21)*. Gifford and Gillott did the standard dimensional change tests for OPC and alkali-activated slag concrete using aggregate from six sources in Canada, and they suggested that alkali activated slag concrete are less susceptible to deleterious expansion due to ASR compares to OPC *(22)* . Wang concluded that AAS concrete suffers no AAR because hydration products bind 80% of the alkali at one year *(23)*. Additionally, Garcia-Lodeiro found that alkali activated fly ash concrete has smaller ASR expansion compares to that of OPC under test method ASTM C1260, and they also proved that calcium plays a vital role during the ASR gel expansion process *(24)*. Conversely, Bakharev found that alkali activated slag concrete exhibited higher expansion compared to OPC under the long-term test method ASTM 1293, and concluded that alkali activated binders system is more vulnerable to ASR compares to OPC *(25)*. With respect to effects of aggregate type, Puertas also indicated that compares to calcareous aggregates, siliceous aggregates are more prone to ASR in alkali-activated mixtures *(26)*. For most of these studies, though differing in exposure conditions, all rely on the linear expansion of mortar or

concrete as an indication of the occurrence of ASR. However, no sound conclusions could be gathered from the literature, and so the topic of the susceptibility of AAC to deleterious ASR remains debatable.

1.4 Research significance

Despite numbers of studies characterizing the ASR of portland cement binders, comparatively little investigations of the ASR of alkali-activated fly ash and slag binders have been performed. This study seeks to address the uncertainty of ASR in AAC, and to investigate the mechanism of ASR in AAC. Additional to that, another focus of this investigation is to assess the effectiveness of existing ASTM test methods in identifying the occurrence of ASR in alkali activated concrete.

1.5 Objectives

Specifically, the objectives of this study are to;

   I.   Evaluate the susceptibility of deleterious ASR in AAC concretes made with both non-reactive aggregates and those known to be highly alkali-silica reactive.

  II.   Investigate the effectiveness of existing ASTM test methods in identifying the occurrence of ASR in alkali activated slag and fly ash (AAC) concrete.

 III.   Quantify the ASR expansion kinetics of AAC under influence of different parameters including aggregate type, activator type, activator concentration and solution to binder ratio.

 IV.   Derive the fundamental mechanisms for ASR in AAC by scanning electron microscopic and EDS analysis

2. Methodology

2.1 Materials

Three binder materials including ordinary portland cement, class C fly ash and slag cement were used in this study. Type-I ordinary portland cement meeting the specifications of ASTM C150 was used for control mixtures. Grade-100 ground granulated blast furnace slag meeting the specifications of ASTM C989 and class-C fly ash meeting the specifications of ASTM C618 were used for alkali-activated binders and concrete. The chemical oxide compositions of these three binders are presented in Table 1.

Table 1 Composition of raw binders

Oxide	Composition (% mass)		
	OPC	Slag cement	Class C Fly ash
CaO	65.00	39.10	21.1
SiO$_2$	21.10	37.80	40.7
Al$_2$O$_3$	6.20	7.91	21.2
MgO	1.60	10.30	4.0
Na$_2$O	0.09	0.30	1.5
Fe$_2$O$_3$	2.90	0.43	5.4
SO$_3$	2.00	2.60	2.4
K$_2$O	0.30	0.47	0.6

The activator materials used in this study were sodium hydroxide and sodium silicate. The sodium silicate activator was a compound aqueous solution of sodium silicate (Na$_2$O + M_s·SiO$_2$, where M_s is the silica modulus) and sodium hydroxide (NaOH) diluted in deionized water. Sodium silicate was in the form of a premixed reagent-grade solution which 26.5% Si$_2$O and 10.6% Na$_2$O by mass. Sodium hydroxide was in the form of United States Pharmacopeia (USP)

food grade pellets of 99% purity. The concentration of the sodium silicate activator was specified by the silica modulus (M_s, or the mass ratio of silica to sodium oxide) and the sodium oxide dosage (%Na_2O, by mass of binder). The concentration of sodium hydroxide activators was specified by molarity. Activator solutions were prepared at least 24 hours in advance of use to allow for adequate dissolution and thermal stability. Additionally, an 8M sodium hydroxide solution was also used as an activating solution.

Two types of fine aggregates were used for this study; both were fine aggregates meeting the gradation requirements of ASTM C1293 and ASTM C1567. The first aggregate was a natural quartz-based sand sourced in Potsdam, NY, USA, sieved to the required gradation, and known to be essentially non-reactive in OPC concrete. The second aggregate was a Spratt siliceous limestone aggregate sourced in Ottawa, ON, CA, mechanically crushed, sieved to the required gradation, and known to be highly alkali-reactive in OPC concrete. The coarse aggregate used in method ASTM C1293, sourced from Potsdam Stone & Ready-Mix in Parishville, NY, was a quarried crushed stone composed mainly of limestone.

2.2 Sample Preparation

Concretes were mixed and cast in accordance with the specifications of ASTM C192. Concrete and mortar were mixed in a variable speed bench mixer. The binder materials and aggregates were first charged into the mixing vessel and thoroughly mixed for one minute. The activator solution was then added and the batch was mixed for two minutes at high speed. For test method ASTM C1567, mortar was cast into standard mortar bars measuring 25.4 x 25.4 x 254 mm (1.0 x 1.0 x 10 in) in two lifts and consolidated with the aid of a vibrating table. Similarly, for test

method ASTM C 1293, concrete was cast into prismatic specimens measuring 50.8 x 50.8 x 254 mm (2.0 x 2.0 x 10 in). Once cast, specimens were trowel-finished and sealed in plastic to limit moisture loss. Henceforth, specimens were cured at either ambient or elevated temperature according to its corresponding curing condition. Those cured at ambient temperature were stored at 23±2 ℃ and >95 %RH for the prescribed duration. Those cured at elevated temperature were stored in a laboratory oven at 50±2 ℃ for 48 hours. A minimum of four prisms were cast for each type of concrete.

2.3 Mixture Proportion

Alkali activated slag and fly ash concrete/mortar mixtures were evaluated in this study. Sixteen AAC mixtures with normal non-reactive aggregates and two mixtures with Spratt reactive aggregates (Rx) were investigated in this study. Two portland cement mixtures, one with non-reactive aggregate (Non- Rx) and another with reactive aggregate, were also evaluated as references. The mixture proportions are detailed in Table. 2. The solution-to-binder ratio (s/b) is the mass ratio of activator solution to binder.

Table. 2 Mixture proportions (activators and curing conditions)

Mixture	Binder	Aggregate	Na$_2$O (% binder mass)	$M_s = \dfrac{SiO_2}{Na_2O}$	s/b	Curing condition
S1		Non-Rx	4.0	0.75	0.40	
S2		Non-Rx	5.0	0.75	0.40	
S2-Rx		Rx	5.0	0.75	0.40	Ambient (23 ± 2℃)
S3		Non-Rx	4.0	1.5	0.40	
S4	Slag cement	Non-Rx	5.0	1.5	0.40	
S5		Non-Rx	5.0	1.5	0.45	
S6		Non-Rx	5.0	1.5	0.50	
S7		Non-Rx	N/A (8M NaOH)		0.45	
S5-H		Non-Rx	5.0	1.5	0.45	Elevated (50 ± 2℃)
S7-H		Non-Rx	N/A (8M NaOH)		0.45	
FC1		Non-Rx	4.0	1.5	0.40	
FC2		Non-Rx	5.0	1.5	0.40	
FC2-Rx		Rx	5.0	1.5	0.40	Ambient (23 ± 2℃)
FC3	Class C fly ash	Non-Rx	6.0	1.5	0.40	
FC4		Non-Rx	5.0	1.5	0.45	
FC5		Non-Rx	5.0	1.5	0.50	
FC4-H		Non-Rx	5.0	1.5	0.45	Elevated (50 ± 2℃)
FC6-H		Non-Rx	N/A (8M NaOH)		0.45	
OPC	OPC	Non-Rx	N/A	N/A	0.40	Ambient (23 ± 2℃)
OPC-Rx	OPC	Rx	N/A	N/A	0.40	

2.4 Experimental method

2.4.1 Alkali-Silica Reactivity under ASTM C1293 and ASTM C 1567

Alkali-silica reactivity was measured in accordance with two standard test methods: ASTM C1293 and ASTM C1567. Both methods involved the preparation of prismatic specimens with embedded gage studs. Linear expansion of specimens was taken as evidence of the occurrence of ASR. Under test method ASTM C1293, concrete prisms (as previously described) were cured for 48 h. The initial length, mass, and dynamic modulus of elasticity was recorded. Specimens were then stored vertically over water in sealed containers with wicking liners at 38 ℃ (100 ℉) and

the length, mass, and dynamic modulus of elasticity were recorded periodically for 1 year. Measurements were taken daily for the first week and then at increasing intervals thereafter. Under test method ASTM C1293, expansions greater than 400 µε (0.04%) are suggestive of potential deleterious ASR.

Test method ASTM C1567 is a shorter term test which involves the exposure of mortar to more aggressive conditions that those required by ASTM C1293. Mortar bars (as previously described) were prepared and cured for 48 h. Specimens were then demolded and stored in a water bath at 80 ℃ for 24 h. The initial length, mass, and dynamic modulus of elasticity was recorded. Specimens were then stored submerged in a 1 N solution of sodium hydroxide at 80 ℃ for 14 d. The length, mass, and dynamic modulus of elasticity was recorded immediately following this submersion period. Under test method ASTM C1567, expansions greater than 1000 µε (0.1%) are suggestive of potentially deleterious ASR.

2.4.2 Dynamic Modules of Elasticity (DME)

Dynamic modules of elasticity (DME), known to be very sensitive to the formation of cracks, was used to evaluate the deterioration in concrete and mortar specimens. The dynamic modulus of elasticity was measured by the resonant frequency method in accordance with the specifications of ASTM C215. In most cases for OPC system, the cracking associated with ASR results in a marked reduction in the resonant frequency and dynamic modulus of elasticity. These reductions are typically not observed in the first few months of testing, but generally become apparent within one year.

2.4.3. Scanning Electron Microscopy (SEM)

Scanning electron microscopy (SEM) was used as a petrographic way to examine the uncertainly of ASR developed in AAC. Microstructure of samples was studied under the secondary mode of

SEM (SSEM) and backscattered mode of SEM (BSEM) after specific exposure period. To prepare the SSEM samples, the samples were cut into small cubes, freeze-dried using liquid nitrogen and vacuum desiccated, following the aforementioned exposure period. Prior to examination under the SSEM, the small cubes were snapped to expose a free fractured surface and sputter coated. For BSEM examination, the samples were cut into size (around 2 cc) by using a diamond slow speed saw and submerged in 2-propanal for 3 days to quench their hydration. Then, the samples are dried in an oven at 50℃ for 3 days. After that, specimens were impregnated with epoxy and polished using 45 µm and 15 µm lapping pads. Diamond paste with particle size ranging from 9 µm to 0.25 µm are applied on the lapping cloth during polishing. Polished specimens are placed in vacuum desiccators until being examined using BSEM. Shortly prior to the characterization, the polished samples are sputter coated with 60%Au/ 40% Pd.

2.4.4 Energy-Dispersive X-ray Spectroscopy (EDS)

In order to help understand the mechanism of ASR in alkali activated binders from the quantitative point of view, an Oxford instruments INCA system was used for energy-dispersive X-ray spectroscopy (EDS) along with SEM examination. For each sample, twelve points were selected in specific locations and the representative chemical composition results were analyzed in the study.

2.4.5 Internal Relative Humidity (Internal RH)

Modified ASTM F2170 was employed to measure the internal relative humidity of alkali activated slag or fly ash concrete. Internal RH sensors were embedded in 2 by 4 inches mortar at a depth of 2 inches during casting. The internal RH measurements commenced immediately after setting time at a frequency of hourly up to 24 hours followed by each measurement daily up to 56 days. During the curing period, the cylinders remained inside the closed plastic molds. The

measurements at depth were duplicated for each specimen to check repeatability. The sensors incorporated factory calibration to within ±1.8% RH (±3% when over 90% RH).

2.4.6 Pore Solution Analysis

Traditionally, the pore solution from a hydrating cementitious system is extracted by vacuum filtration before setting and by using a high-pressure extraction method after setting using Barneyback and Diamond's method. The pressure needed for extracting pore solution from alkali-activated concrete found to be very high. Hence, a traditional pore solution extracting press fabricated at Clarkson was not useful. Instead, a modified method was used for studying the pore solution chemistry. Alkali activated slag and fly ash pastes with a high solution to binder ratio were used. Since the setting was delayed in such a high water content system, a vacuum filtration method for expressing pore solution periodically over a period of 8 hours can be used. The solution to binder ratio is maintained at 2 for every paste. After the specific hydration time, pore solution was extracted using vacuum filtration under pressure. The solution is extracted using the filter paper with 0.2μm pore size. The extracted pore solution was analyzed by an inductively coupled plasma spectroscopy (ICP-MS) method

3. Results and discussion

3.1 Expansion strains, mass change and dynamic modulus of elasticity

3.1.1 Effects of Binder and Aggregate Type

The linear expansion, change in mass, and dynamic modulus of elasticity of AASC, AAFC and OPC concrete with non-reactive and reactive aggregate under long-term ASTM test method C1293 are shown in Fig.2. In general, AAS has much higher expansion compared to those in FC

and OPC. The expansion of AAS samples all exceed the limit of 400 µε by one-year age; while the expansion in FC and OPC was still well below the limit unless with reactive aggregate. Furthermore, irrespective of the binder type, the shape of the expansion curve was different between aggregate types. At early age, the expansion in AASC concrete was more rapid than in FAC and OPC concrete, irrespective of aggregate type. For both binder types, the expansion in specimens with reactive aggregate was similar to that in specimens with non-reactive aggregate

(a) Expansion

(b) Mass increase

(c) Dynamic modulus of elasticity
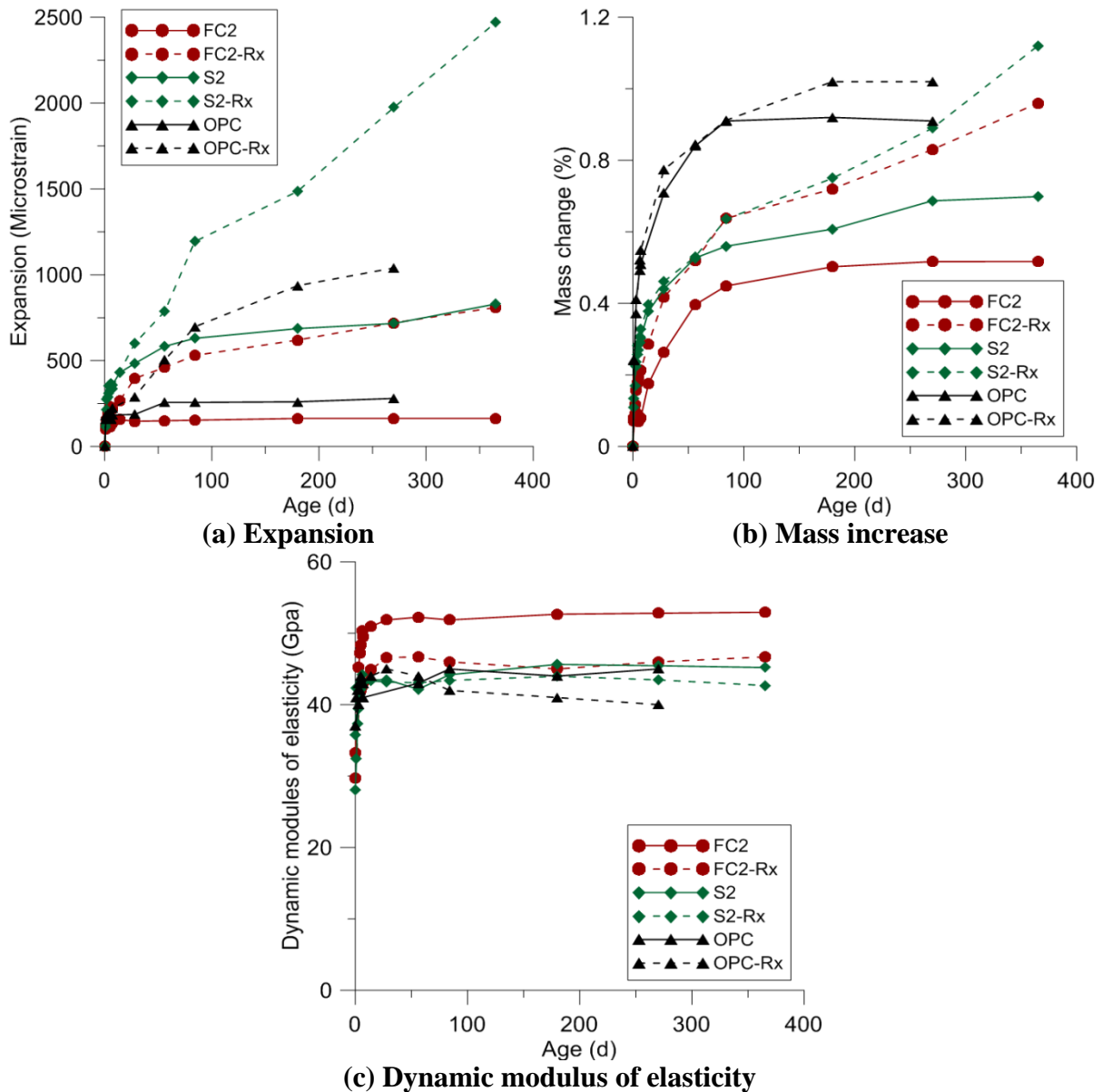
Fig. 2 Effect of binder and aggregate type on ASR of AASC, AAFC and OPC under ASTM C1293 test

18

at early age. However, the expansion with non-reactive aggregate tended to subside after 28 day that with reactive aggregate continued to increase steadily. Additionally, the expansion of OPC concrete was only increased to 250 µε in the first 50 days and then remained nearly constant, while OPC-Rx had a much higher expansion around 1000 µε with a more rapid increase in trend by the end of 250 days.

For concrete with reactive aggregate, the excessive expansion may be due to the expansion of ASR gels inside the sample, and this is consistent with its mass increase and dynamic modules of elasticity change. Similarly, to the expansion trends, the mass change of all the concrete increased very rapidly in its first 50 d. After that, the mass change of none-reactive concrete remained nearly the same, while mixtures with reactive aggregate increase steadily. This is mainly because these samples with reactive aggregate may have more chance to form ASR gel, and has a higher ability to absorb water from external environment. The trend in dynamic modulus of elasticity was similar in AASC concrete with both aggregate types; similarly, in the case of OPC and AAFC, the dynamic modulus of elasticity was slightly lower while reactive aggregate was used in the mixture.

(a) Expansion   **(a) Mass change**
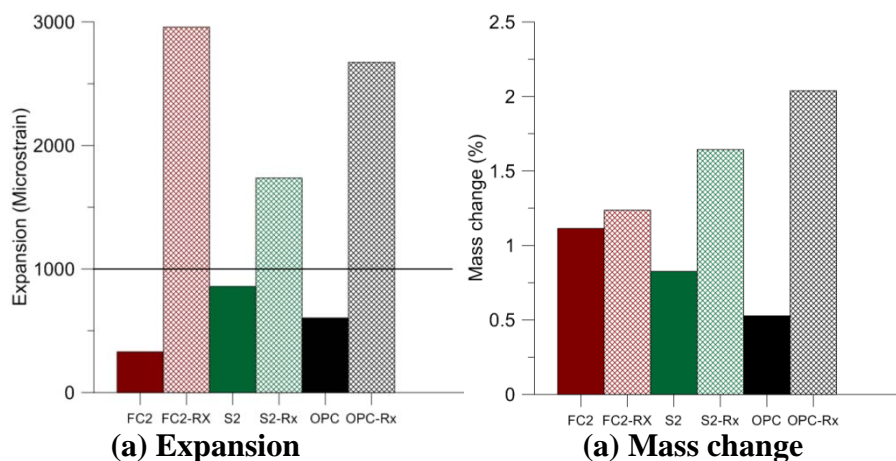
Fig. 3 Effect of binder and aggregate type on ASR of AASC, AAFC and OPC under ASTM C1567 test

Under the more aggressive short term test method ASTM C1567, the expansion of AASC, FC and OPC concrete with non-reactive aggregate was below the limit of 1000 µε as shown in Fig.3; Conversely, the expansion of AASC and OPC concrete with reactive aggregate exceeded this limit by more than 150% and 80%. For samples with non-reactive aggregate, even both values were well below the expansion limit, the expansion in AASC concrete with non-reactive aggregate was noticeably higher than that in FC and OPC concrete with non-reactive aggregate. These results with the petrographic results presented later have shown that ASR did occur in both AAS, FC and OPC concrete while reactive aggregate was used. The reactive silica present in the reactive aggregate was attacked by strong alkalis from the pore solution and resulted in formation of deleterious alkali-silica gel. With the presence of moisture, this alkali silica gel can expand dramatically in the area of gel accumulation, and cause micro-cracks even pop-out. Furthermore, these results suggest that no ASR occurred in either concrete with non-reactive aggregate. The visual appearances indicated that the integrity of the tested specimens retained and no significant cracking was formed on the surface of the sample by the end of 1 year.

This better ASR resistance of the alkali activated system could be attributed mainly to two reasons. Firstly, the lower calcium content in AAC compares to OPC might have played a vital role in inhibiting the deleterious ASR gel formation. It has been generally accepted that calcium (calcium hydroxide) is one of the essential component for the formation of ASR gel in OPC concrete. In the presence of calcium, the general reaction equation was detailed as following:

$$Ca(OH)_2 + SiO_2 + NaOH + H_2O \longrightarrow n_1Na_2O \cdot n_2CaO \cdot n_3SiO_2 \cdot n_4H_2O \text{ (gel-type product)}$$

The better durability of the alkali activated binders may be attributed to its lower calcium C-S-H structure (with Ca/Si<1.0) than OPC paste*(27-29)*. OPC paste has a higher calcium content due to the presence of residual C_3S and C_2S in addition to CH and C-S-H gel, having Ca/Si=1.7*(30)*.

These calcium-based components in OPC could attack the reactive silica in aggregate, forming an expansive gel mostly starting from the edge of aggregate.

Additionally, during the early age of hydration, more than 70% (Fig. 31) of alkali were bound in hydration product, so only very limited alkali was available for ASR reaction. This was also consistent with the petrographic results presented later.

3.1.2   *Effects of Silica Modulus and Sodium Oxide Dosage for AAS*

The linear expansion, change in mass, and dynamic modulus of elasticity of AASC concrete with varying activator concentrations under long-term ASTM test method C1293 are shown in Fig. 4. Similarly, the expansion and mass change of AASC mortar with varying activator concentrations under short-term ASTM test method C1567 are shown in Figure 5. Generally, the expansions of all AASC concretes under ASTM C1293 exceeded the recommended expansion limit of 400 µε, while their expansion under ASTM C1567 was well below the expansion limit of 1000 µε. The expansion under both methods tended to increase with sodium oxide dosage. The expansion, mass change, and dynamic modulus of elasticity continued to increase steadily up to 365 days.

The progressive increase in dynamic modulus of elasticity is likely a result of gradual improvement in the mechanical properties, which is magnified by the elevated temperature and humidity under the test conditions. Under ASTM C1293, there was no readily observable correlation between mass change and expansion or sodium oxide dosage, although the mass change under ASTM C1567 was inversely correlated to expansion and sodium oxide dosage.
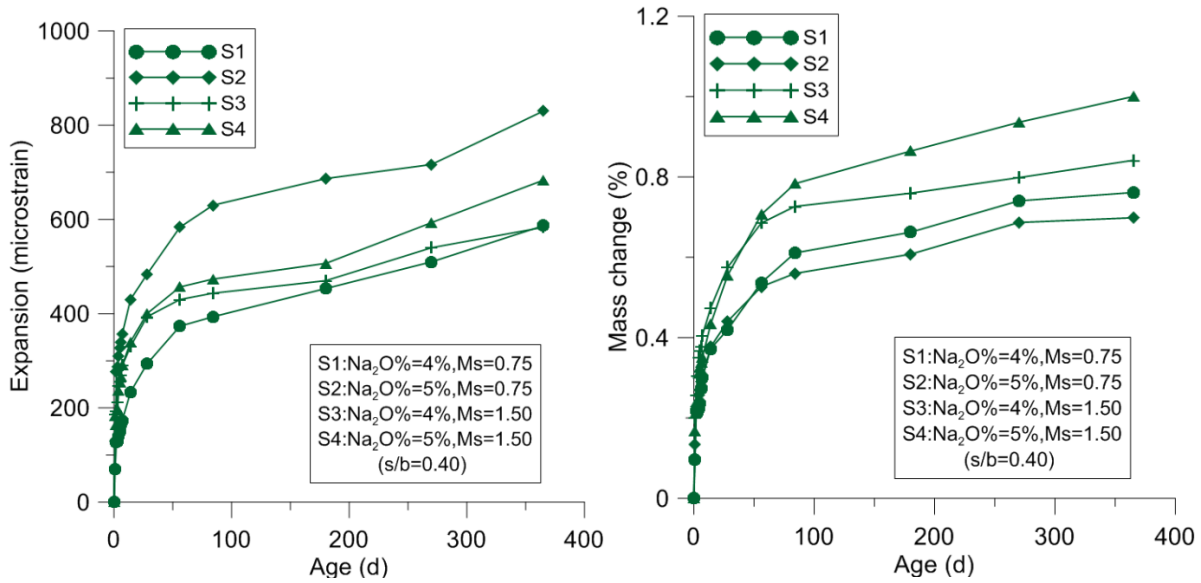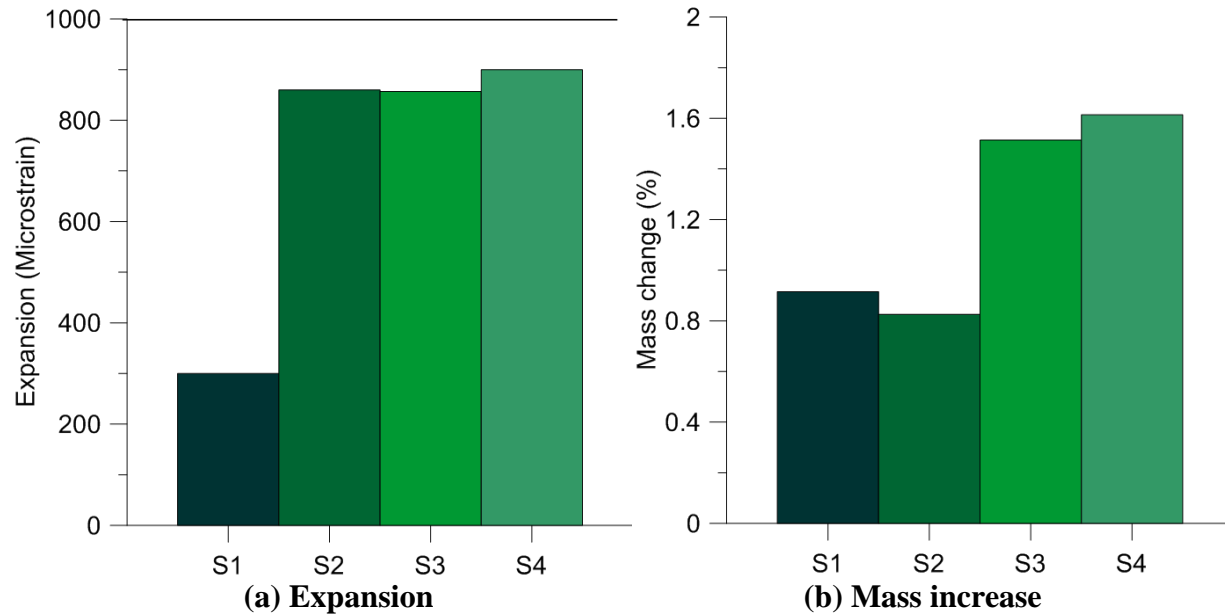
(a) Expansion **(b) Mass increase**
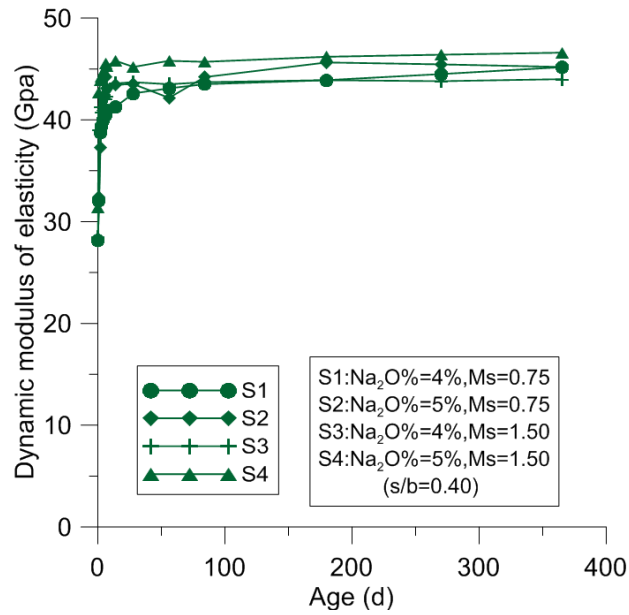
**(c) Dynamic modulus of elasticity**

Fig.4 Effect of silica modulus and sodium oxide dosage on ASR of AASC under ASTM C1293 test

Fig. 5 Effect of silica modulus and sodium oxide dosage on ASR of AASC under ASTM C1567 test

The lack of reduction in dynamic modulus of elasticity, and the lack of mechanical degradation that it suggests, indicates that the observed expansion is likely not due to ASR but instead to some other phenomenon. The excessive volume change observed here was probably result of poor volume stability, or increased water absorption capacity due to the decreased internal humility for AASC. The internal relative humidity (RH) of AASC and FC were measured separately (not undergone the ASR test but just the hydration) and presented with the mass change (water absorption) in Fig.6. It can be seen that the internal relative humidity in AASC was dramatically decreased from about 95% to less than 75% at 56 days, while the RH increased and remained constant at 99% in the case of FC. On the contrary, approximately two times higher mass gain was found in AASC compared to that of FC. The increased water absorption of the slag mixture could be attributed to the very low internal humidity measured in in AASC. This increased water absorption capacity in AASC might be the potential reason for the excessive expansion occurred during ASTM C1293. Additionally, slag mixtures experienced very high autogenous shrinkage during the initial hours of hydration, even before subjecting the samples to

ASTM C1293 tests. The lower internal relative humidity and high autogenous shrinkage might have caused the excessive expansion upon exposure to high relative humidity.
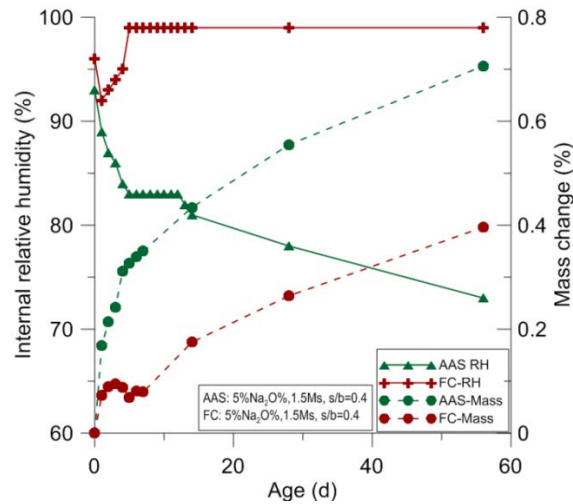
Fig. 6 The internal relative humidity and mass change under ASTM C1293 of alkali activated slag and fly ash concrete.

Fig. 7 shows the expansion strain, change of mass and dynamic modules in FC concrete specimens with various concentration of sodium silicate activator when subjected to ASTM C1293 test. It is clear that expansions in FC specimens were all below the limit of 400 με under ASTM C1293, while the expansion of two mixtures exceeded the limit of 1000 με in the short-term ASTM C1567 test. Furthermore, the FC concrete expansions and mass change were all decreased for almost 40% when Na_2O% increased from 4 or 5% to 6%. These are likely a result of mechanical strength improving effect while higher sodium content activator. The dynamic modulus of all the FC concrete steadily increased up to around 50 GPa in the first 20 days then remained constant, and the results also showed that the elastic modules of FC concrete was not affected by the increased alkali content in the solution.

Similar to AAS, the accelerated test results and long-term test results presented here reveals a certain amount of disagreement between each test method. However, the steadily increased dynamic modules of elasticity over time likely indicate the absence of extensive cracking or the

disintegration of the samples. Hence, the ASTM C1293 test along with the dynamic modulus elasticity measurement may be adequate to determine the ASR reactivity of these samples. Also, it appears that the amount of Na$_2$O content can influence the expansion and mass change, but It is difficult to conclude that these parameters affect the alkali-silica reactivity significantly.

(a) Expansion   (b) Mass increase

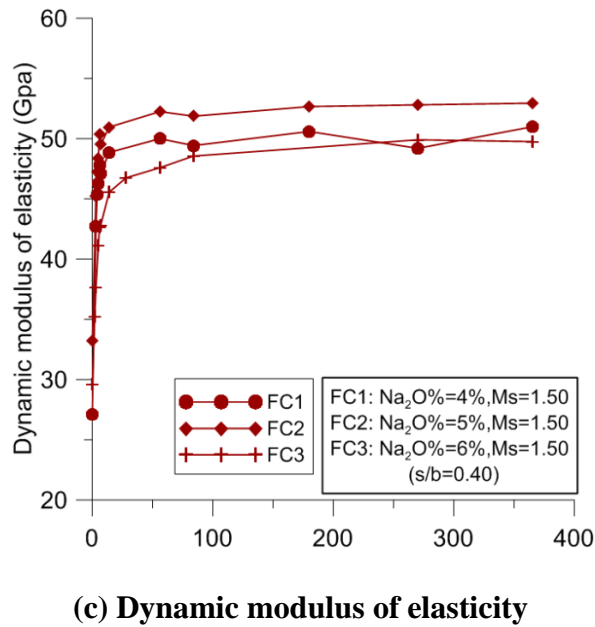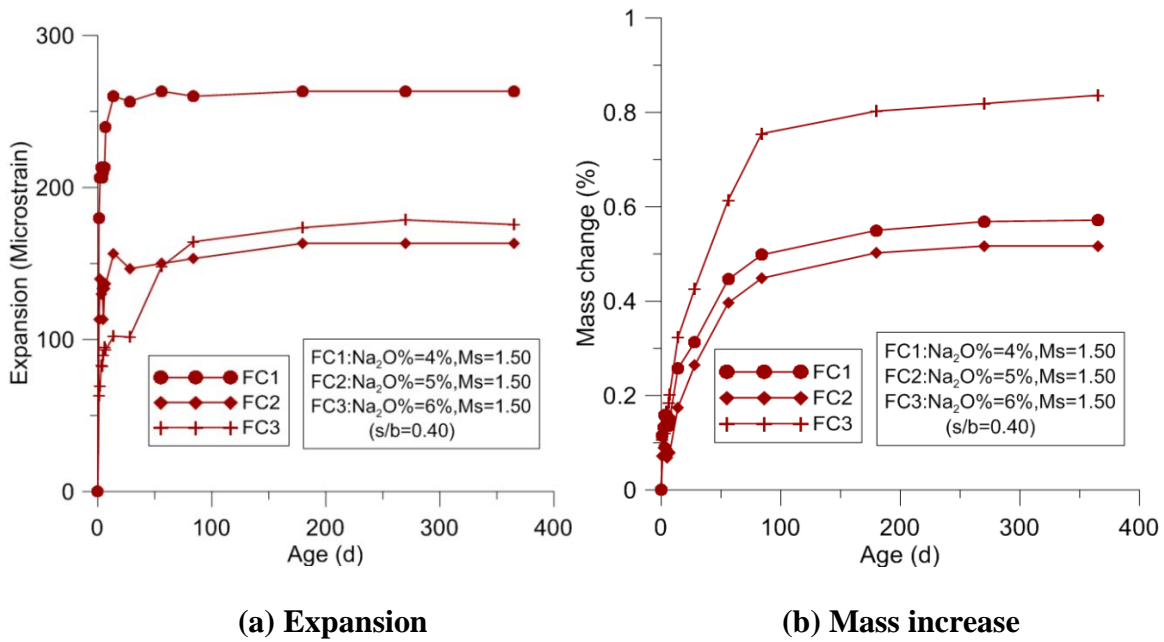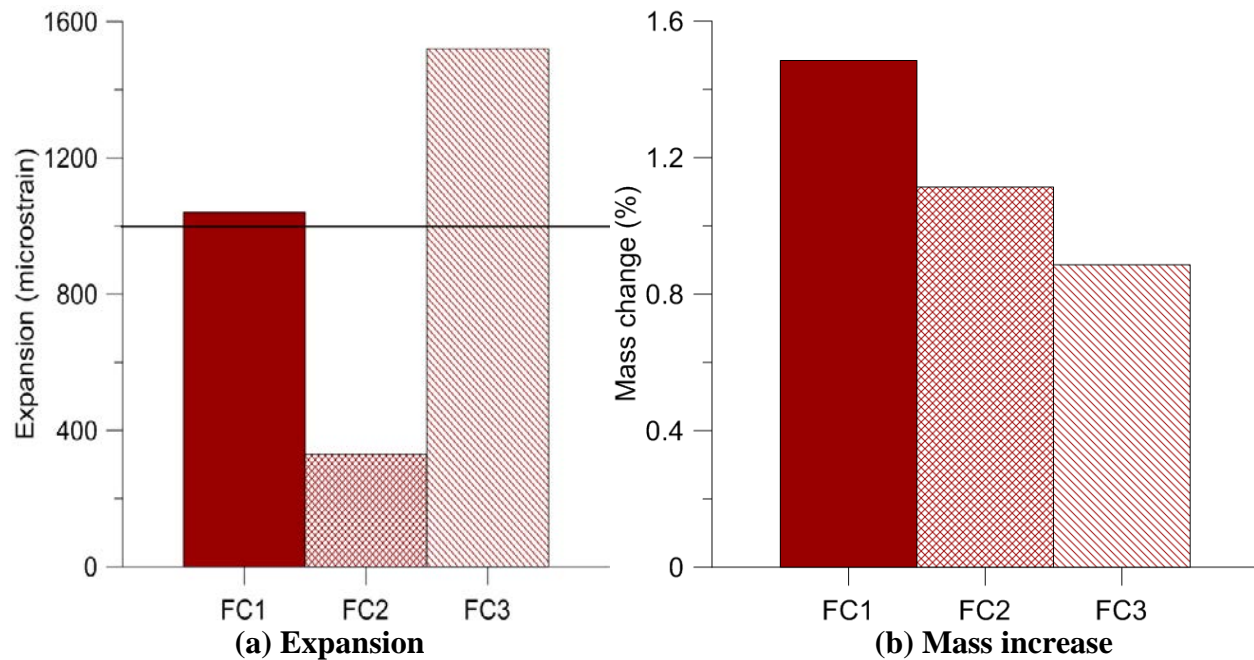(c) Dynamic modulus of elasticity
Fig.7 Effect of silica modulus and sodium oxide dosage on ASR of AAFC under ASTM C1293 test

(a) Expansion　　　　**(b) Mass increase**

Fig.8 Effect of silica modulus and sodium oxide dosage on ASR of AAFC under ASTM C1567 test

3.1.3　Effects of Solution to Binder Ratio

Fig.9 and 10 show the effect of different solution to binder ratio on expansion, mass change and dynamic modulus of elasticity of alkali-activated slag concrete (AASC) subjected to both ASTM C1293 and ASTM C1567. Under test method ASTM C1293, there is no clear trend observable in the figure. Specifically, the expansion level was increased while the solution to binder ratio increases from 0.4 to 0.45 and decreased with solution to binder ratio increases from 0.45 to 0.50. In general, the expansions of all mixtures exceed the limit of 400 macrostrains after 200 days of exposure under test method ASTM C1293, while the expansions in ASTM C1567 shown in Fig.10 are all within the limit of 400 macrostrains by the end of experiment. The excessive expansion observed here also could be due to the unstable stability during the early hydration days as explained earlier in Fig.6
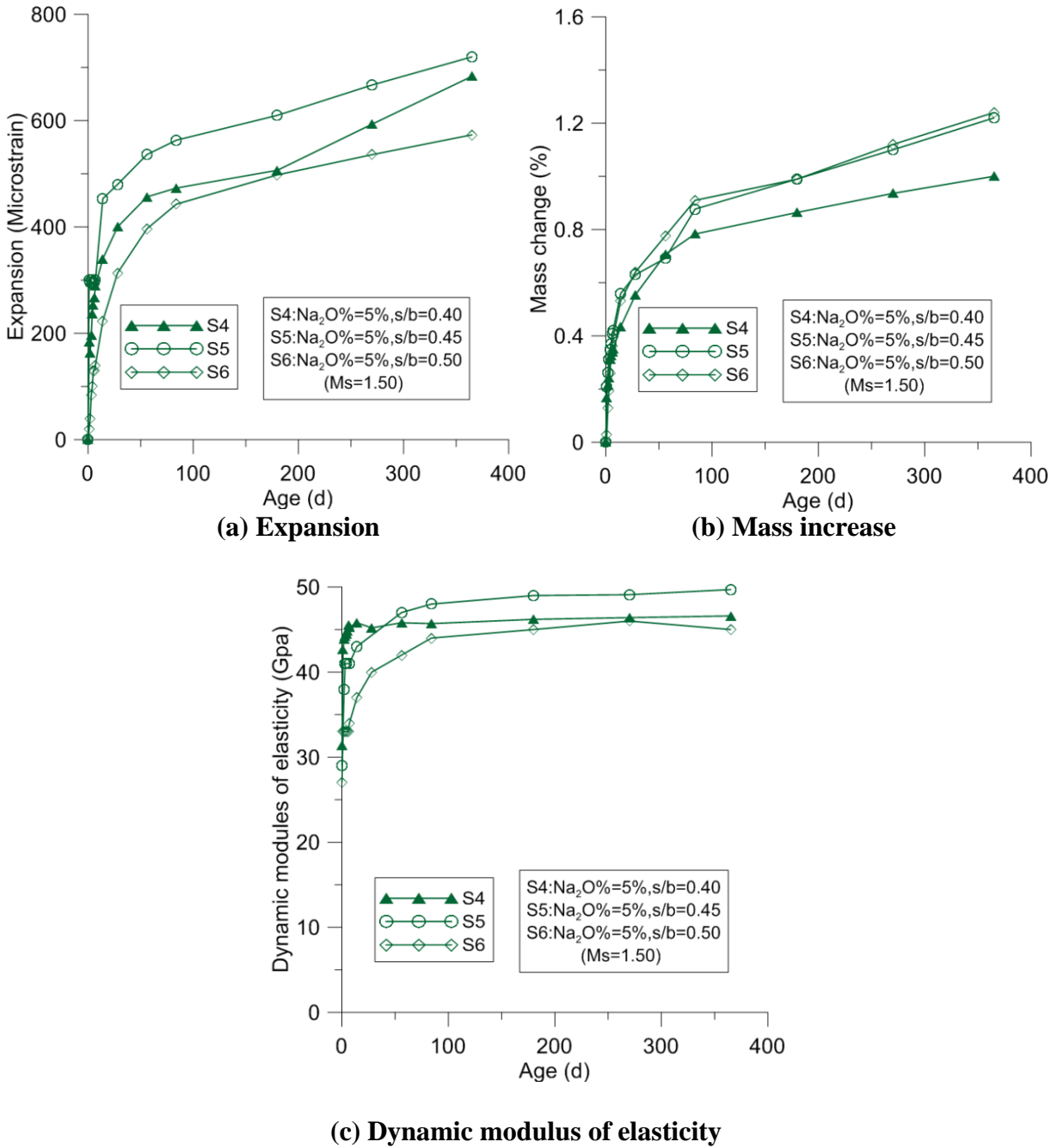
26

(a) Expansion

(b) Mass increase

(c) Dynamic modulus of elasticity

Fig.9 Effect of solution to binder ratio on ASR of AASC under ASTM C1293 test
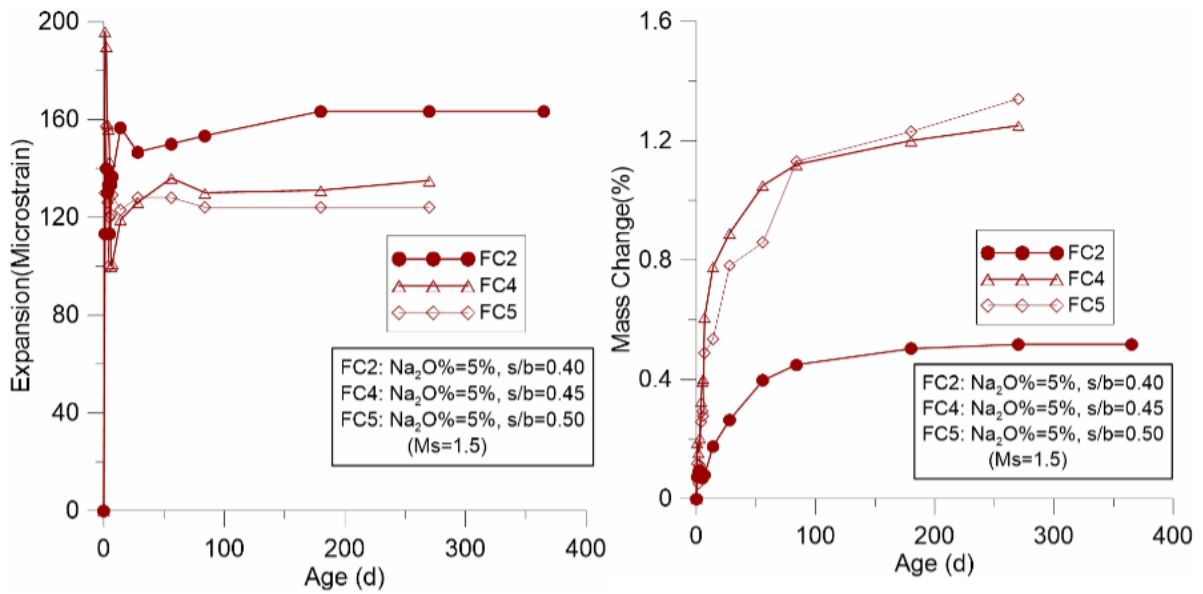
(a) Expansion　　　　**(b) Mass increase**
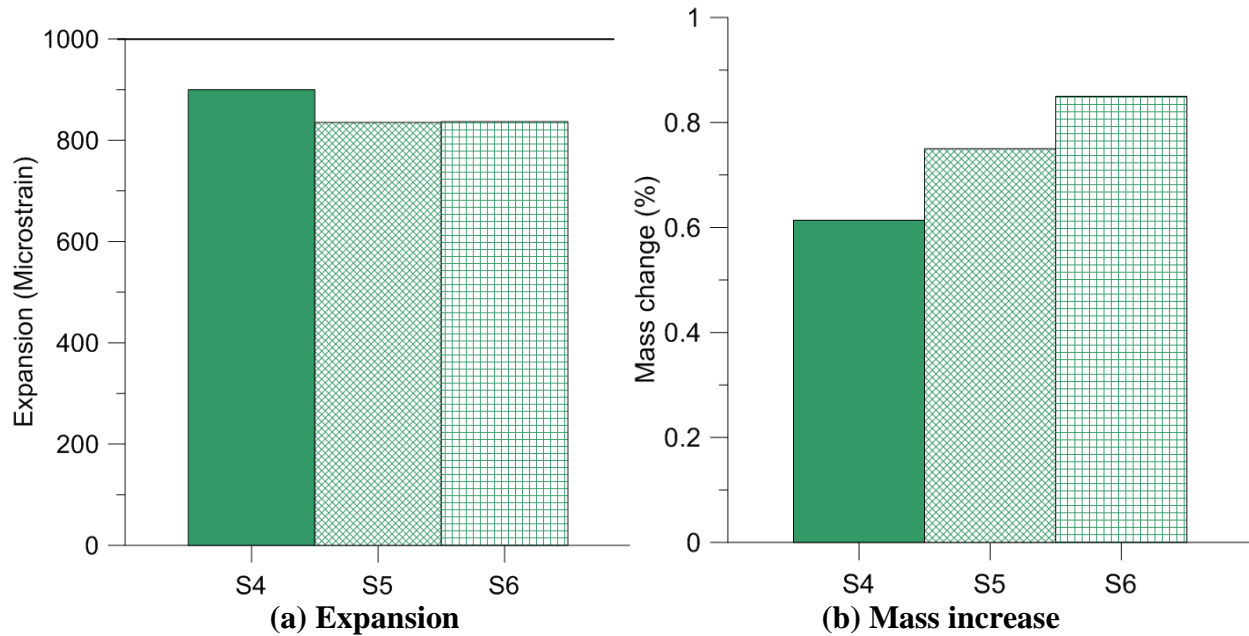
Fig.10 Effect of solution to binder ratio on ASR of AASC under ASTM C1567 test

The influence of solution to binder ratio on the linear expansion, mass change and dynamic modulus of elasticity of alkali activated fly ash concrete (AAFC) under test method ASTM C 1293 and ASTM C1567 are shown in Fig.11 and 12. Generally, the expansions are all below the limit, the expansion strain of alkali activated fly ash concrete in both test method increased significantly with the solution to binder ratio increases from 0.4 to 0.5. This may result from a decreased OH⁻ concentration due to the increased water content within the pore solution, which could inhibit ASR. Similar to the expansion trend, for both test methods, the mass change of alkali activated fly ash concrete increased with higher solution to binder ratio. The potential reason for this mass gain is mainly due to the increased porosity and water absorption capacity of higher solution to binder ratio mixtures.

Additionally, it can be seen that the modulus of elasticity decreased with an increase in solution to binder ratio. This is expected even in OPC system, lower water to cementitious materials ratio (w/cm) lead to better DME.

(a) Expansion

(b) Mass increase
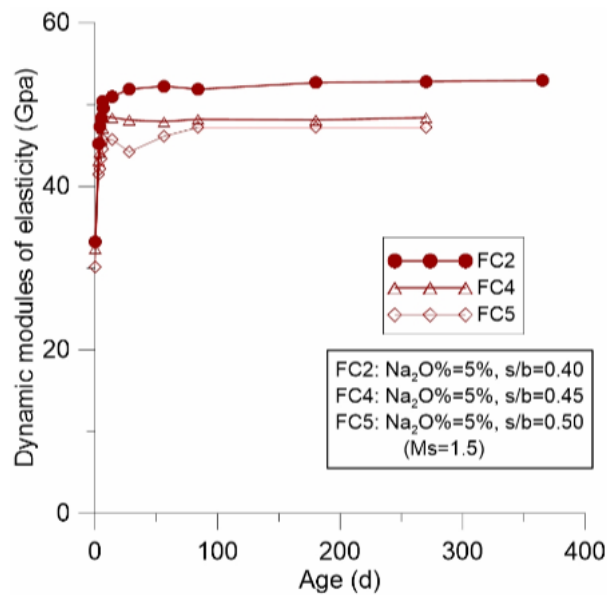
(c) Dynamic modulus of elasticity
Fig.11 Effect of solution to binder ratio on ASR of AAFC under ASTM C1293 test

(a) Expansion　　　　　　　　　　**(b) Mass increase**

Fig.12 Effect of solution to binder ratio on ASR of AAFC under ASTM C1567 test

3.1.4 Effects of Activator Type and Curing Condition
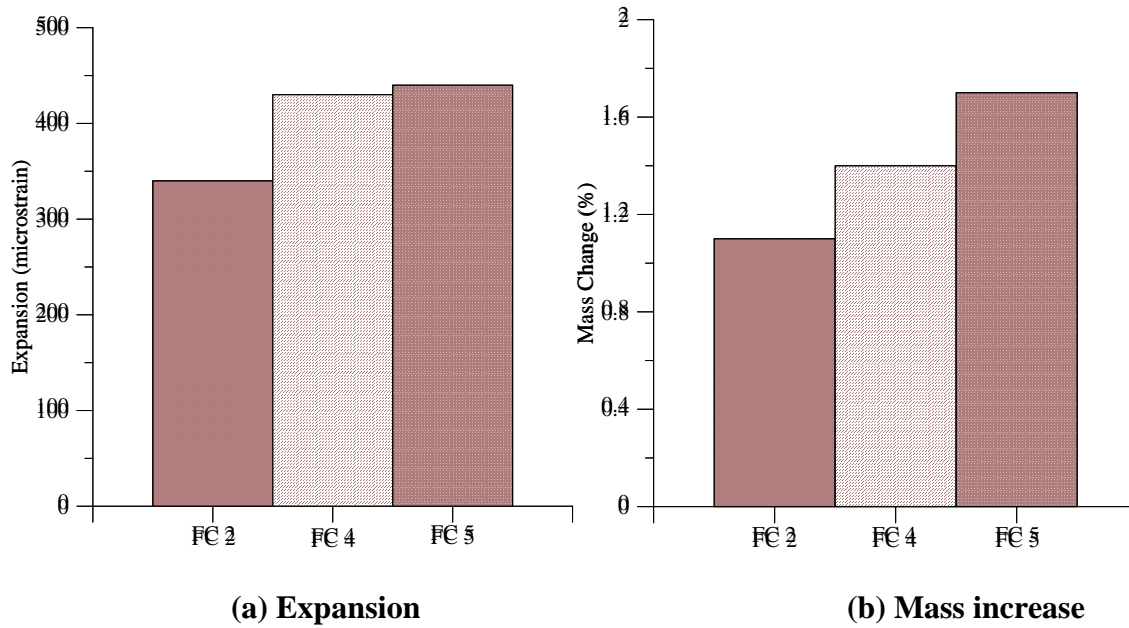
The linear expansion, mass change, and dynamic modulus of elasticity of AASC concrete with varying activator type and curing condition under long-term ASTM test method C1293 and short term ASTM C1567 are shown in Fig.13 and 14 respectively. Although, the mass increase under ASTM C1293 was similar, the expansion was significantly higher with sodium hydroxide as the activator than with sodium silicate. The expansion of AASC concrete activated with sodium hydroxide exceeded the expansion limit by a significant margin; that of AASC concrete activated by sodium silicate exceeded the limit by only a few hundred micro strains. The internal relative humidity of sample S7 showed that the relative humidity was much lower approximately 50% from the setting of these samples to several days during the initial hydration period which is much lower than that of sodium silicate activated slag. The autogenous shrinkage was also high. This volume instability might have caused such a high expansion when exposed to 100% RH under ASTM C1293.

30

(a) Expansion

(b) Mass increase

(c) Dynamic modulus of elasticity
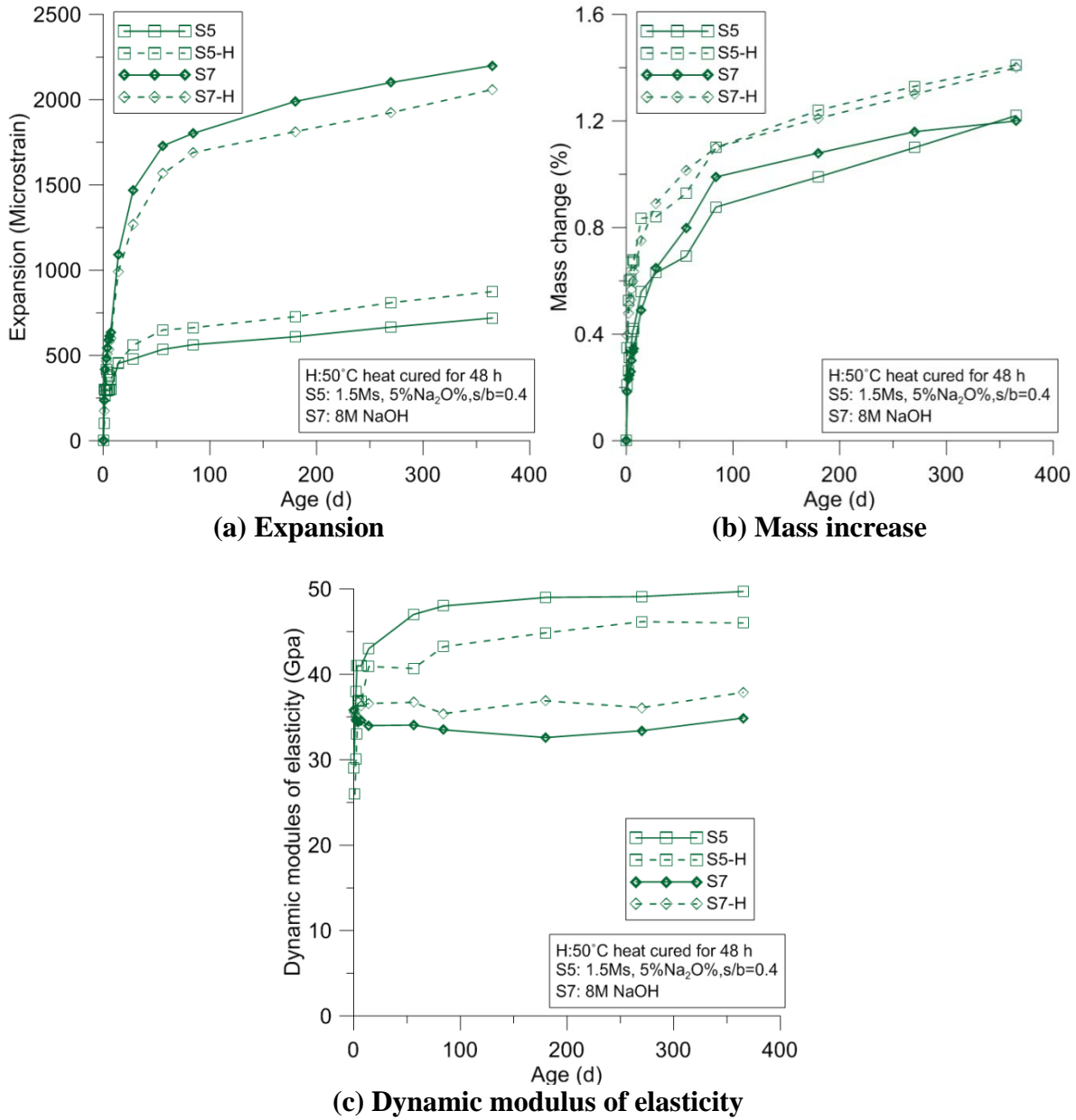
Fig.13 Effect of activator types and curing conditions on ASR of AASC under ASTM C1293 test

Under ASTM C1567, the opposite trend was observed: The expansion of AASC concrete activated by sodium silicate was much higher. There was little difference in the expansion of similar mixtures under ambient and elevated curing conditions. The mass increase was generally higher for heat-cured specimens. This is likely due to the dry condition of heat-cured specimens,

which allows for increased moisture absorption. As per previous discussions, there was no decline in dynamic modulus of elasticity, which would be suggestive of the occurrence of ASR. The dynamic modulus of elasticity was generally higher in heat-cured specimens, which is consistent with previous studies on the mechanical properties of AASC concrete.
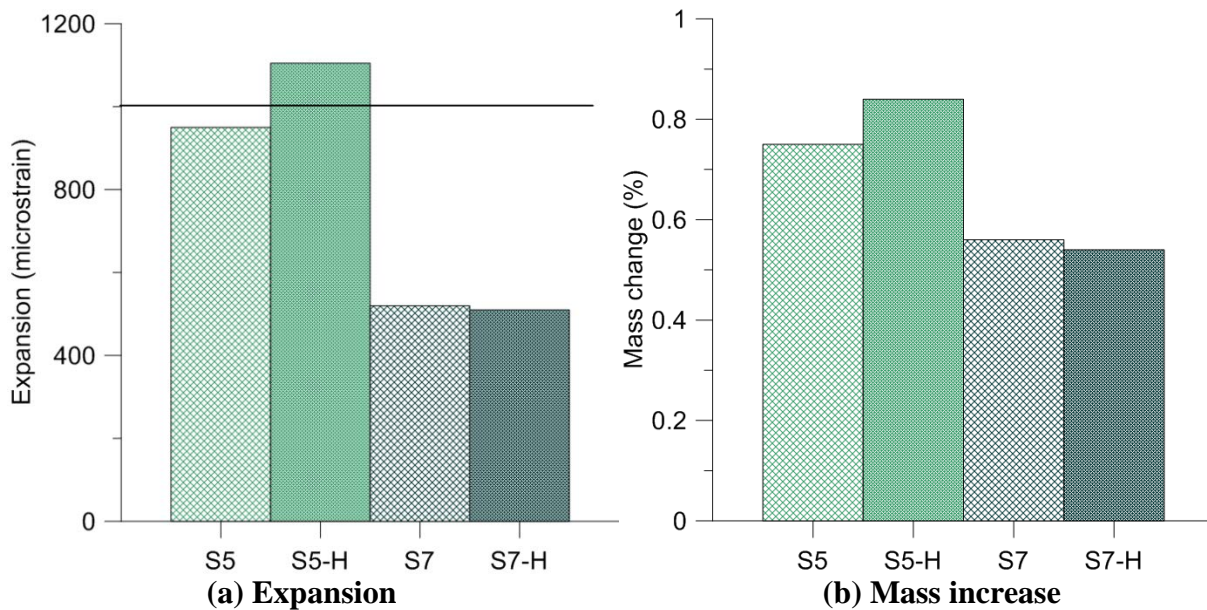
(a) Expansion **(b) Mass increase**
Fig.14 Effect of activator types and curing conditions on ASR of AASC under ASTM C1567 test

In the case of AAFC subjected to test method ASTM C1293, the expansion, mass change and dynamic modules of elasticity with different activator type and curing condition are presented in Fig.15. Generally, under test method ASTM 1293, the linear expansion of heat-cured sodium hydroxide and ambient-cured sodium silicate AAFC specimens are well below half the limit for less than 200 micro-strains, while the expansion of heat-cured sodium silicate activated fly ash concrete is slightly higher than 400 micro-strains. This is likely due to the very rapid hydration rate of heat-cured sodium silicate AAFC may form more micro cracking within the specimen, which allows moisture to have more access to penetrate into samples and causes more expansion immediately after exposing the samples to 100% RH. Moreover, heat cured mixtures appears to

32

have more weight gain as shown in Fig.15, which is mainly due to the fact that the heat curing process can dry out more moisture from the concrete which may increase sample's potential to absorb water later when it is subjected to ASTM C1293 test .

(a) Expansion

(b) Mass increase
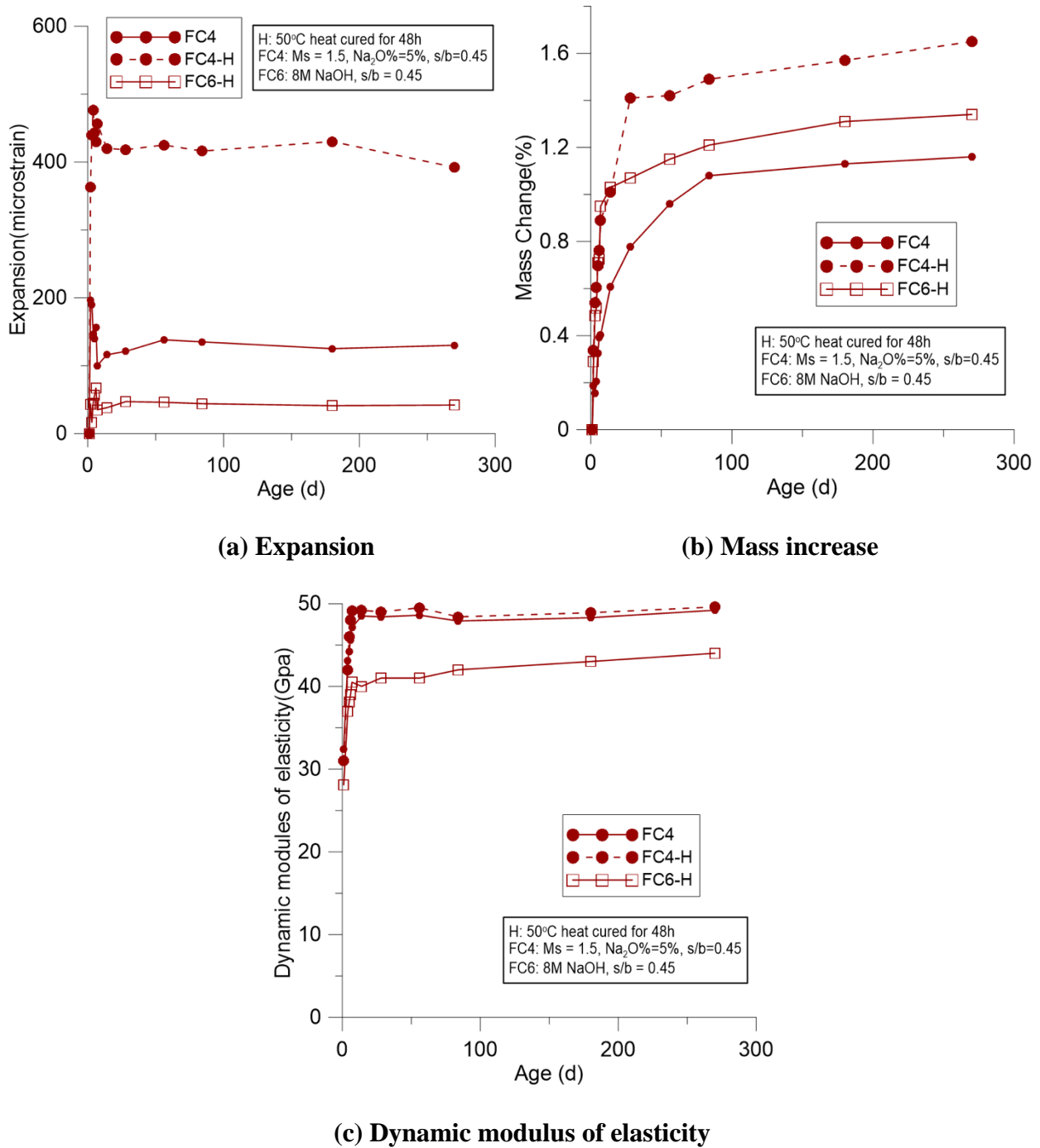
(c) Dynamic modulus of elasticity
Fig.15 Effect of activator types and curing conditions on ASR of AAFC under ASTM C1293 test

The dynamic modules of elasticity trend in Fig.15-c indicate that sodium silicate AAFC has slightly higher dynamic modules of elasticity value than sodium hydroxide AAFC, irrespective of the curing conditions. Additionally, the variation in dynamic modulus of elasticity between each mixture is mainly due to the differences in the compressive strength. Specifically, these mixtures with a higher compressive strength are corresponding to a higher level of dynamic modulus of elasticity.

Fig. 16 shows the linear expansion and mass change of AAFC with various activator types and curing condition while under test method ASTM 1567. Unlike results in ASTM C1293, the expansion of all the mixtures is all within the limit of 1000 macrostrains by the end of the experiment. However, Fig. 16 also indicates that heat-cured specimens appear to have a lower expansion than ambient cured specimens for sodium silicate activated fly ash concrete, and sodium silicate AAFC generally has a higher expansion compares to that in sodium hydroxide AAFC.

(a) Expansion   (b) Mass increase
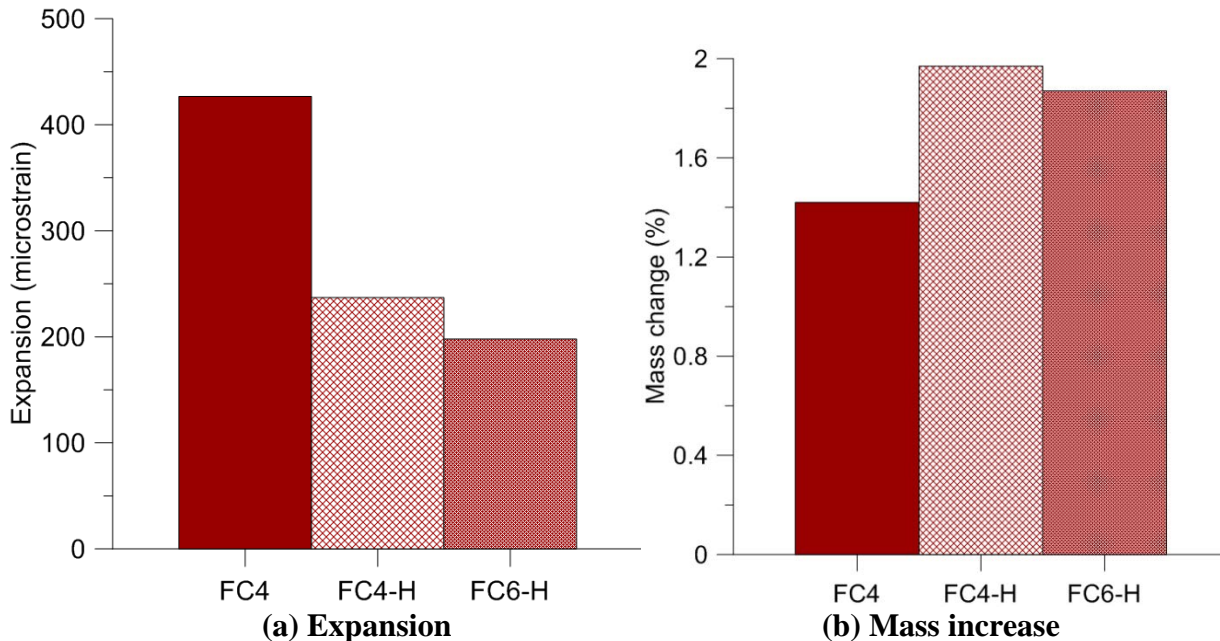
Fig.16 Effect of activator types and curing conditions on ASR of AAFC under ASTM C1567 test

Like test method ASTM C1293, heat-cured specimens likely to have higher mass gain because of its heat curing process might have increased moisture absorption capacity of these samples.

## 3.2 Microstructure and chemical composition

In order to identify the extent of microstructural changes due to the formation of alkali silica gel (ASR Gel), a thorough evaluation of the microstructure under the BSEM mode of scanning electron microscope was undertaken. When deemed suitable, secondary mode images were also collected from fractured samples. The examination included general evaluation of several locations in a sample including paste area, boundary between the aggregate and the hardened paste, aggregate for potential cracking, determination of the presence of gels in the cracks in the paste and in the aggregates. Magnification of an image was chosen to suit the purpose of a particular analysis. First, we discuss the microstructure of a familiar system, sound OPC concrete, followed by an OPC concrete affected with ASR and then the alkali activated systems.

3.2.1 Ordinary Portland Cement Concrete

Fig. 17 shows the microstructure of OPC concrete after six months of exposure to ASTM C 1293 testing conditions. The expansion was less than 200 $\mu\varepsilon$ and as per the standard no deleterious reaction going on in this system. Microstructural evaluation revealed no cracks in the aggregates and only some minor inherent shrinkage cracks occasionally in the paste area. Overall, no signs of ASR reaction.

On the contrary, Fig. 18 shows an OPC concrete (OPC-Rx) with reactive Spratt aggregates. The measured expansion was more than 600 $\mu\varepsilon$ after 180 days of exposure. Apparently, several significant micro cracks were identified within the specimens as displayed in Fig.18 (a) and (b), and most of these microcraking were across the reactive fine aggregate and extended to paste

matrix.   This is mainly because the reactive silica in the sand grain reacts with the alkali contained in the pore solution and forms the deleterious ASR gel inside the aggregate. This ASR gel can expand and causes cracking in the presence of moisture. Finally, the microcracking, normally initiated within reactive aggregate, could grow and develop from sand grain to hardened paste region and lead to deleterious concrete degradation. These results, microstructural investigations for OPC-Rx shown here, are largely consistent with the linear expansion, mass change and dynamic elasticity modulus trend shown in Fig.2. As expected, the Spratt siliceous limestone aggregate is a very reactive aggregate for ASR experiments.
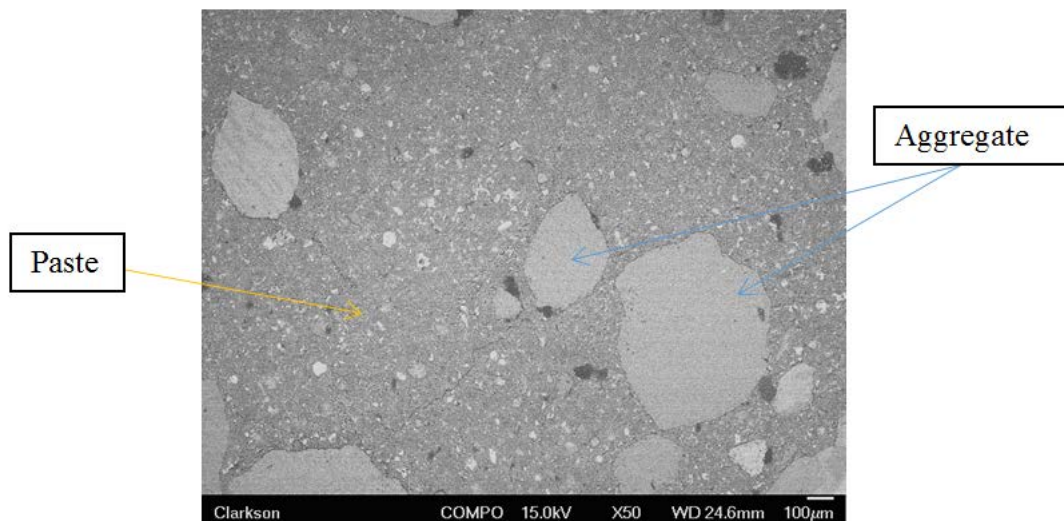
Fig.17 Scanning electron microscopy (Backscattered mode) examination of OPC concrete none-reactive aggregate (OPC) under test method of ASTM C1293 after 6 months.

Fig.18-c is taken at a higher magnification (500x) to see more details of the microstructure, and an EDS analysis (Fig 18 (d)) is also included to show the chemical composition of the ASR gel. It can be seen from the picture that a crack filled with massive and spongy gel, was formed in the aggregate and extended into hydrated hardened cement paste area. The EDS spectrum in Fig.18-d shows that the massive gel found inside the crack is ASR gel, and has a characteristic chemical

composition of silicon (Si), calcium (Ca), sodium (Na)/ potassium (K). The amount of "Ca" may vary depending upon the location of the gel (in the aggregate vs the paste) otherwise the ASR gel has a fixed composition.
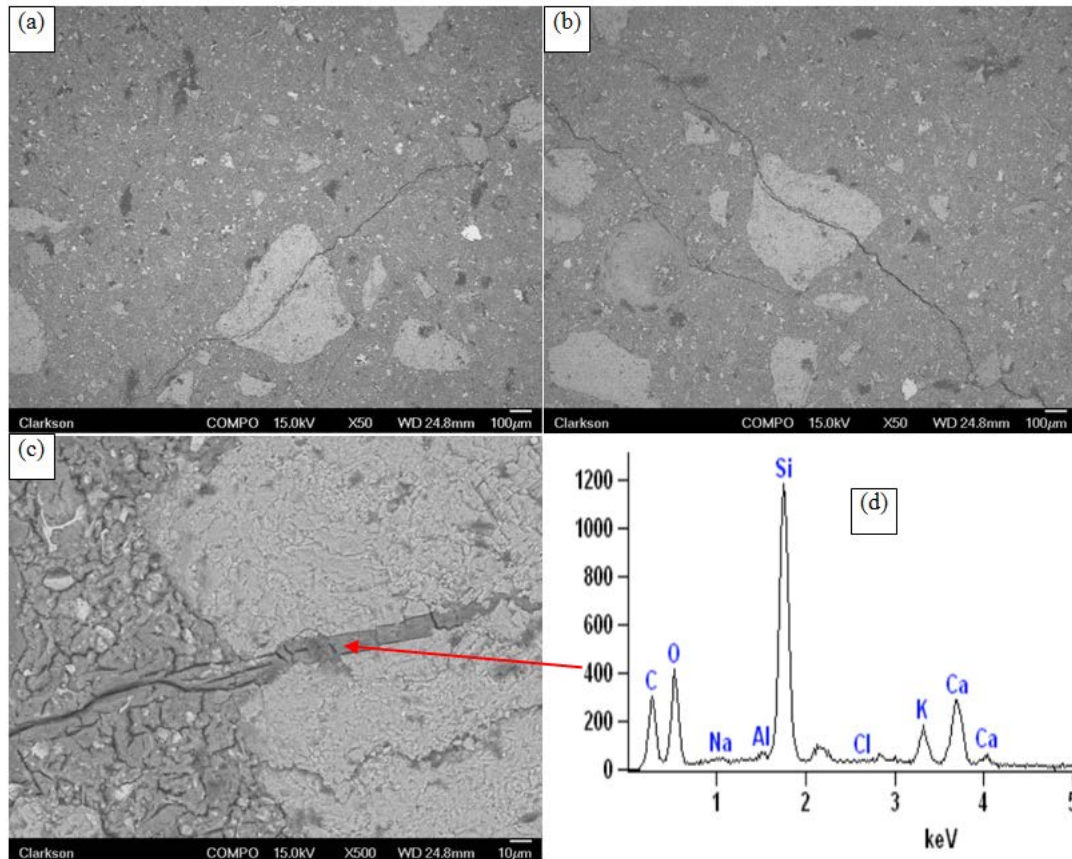
Fig.18 Scanning electron microscopy (Backscattered mode) examination of Ordinary portland cement concrete (OPC-Rx) under test method of ASTM C1293 after 1 year.

3.2.2 Alkali Activated Slag Concrete (AASC)

Fig.19 shows some representative images taken from AASC with none-reactive aggregate (S2) after a one year exposure period as per ASTM 1293 method. In general, dense and consistent microstructure matrix with very few cracks in the paste region and no cracks in the aggregates were found as shown in Fig. 19(a) to (d). This sample (S2) had a strain ~800µℇ, which as per the

ASTM standards indicates the presence of ASR reaction. In spite of the significant expansion experienced by this sample at one year, no signs of ASR reaction (cracks in the aggregate, gel formation) were determined by the SEM or EDS analysis. To verify this, several alkali activated slag concretes with normal non-reactive aggregates (S3, S4, S5 and S7) those experienced expansion beyond the stipulated limit (400 $\mu\varepsilon$) by ASTM 1293 at the end of one year was also examined. Figs 20-23 shows similar analysis as in Fig. 19 for concrete samples S3, S4, S5 and S7 respectively. Some cracks, potentially due to volume instability, can be seen in the paste region of some of these samples but no cracks in the aggregates were found. As shown in Figs.20 (c) &(d) and 23 (e) & (f), the chemical compositions of materials in and around the suspicious microcracking areas were analyzed using EDS in magnified images, and no ASR gel was identified in any of the AASC samples with none reactive aggregate. Additionally, the microcracking in Fig.20 and Fig. 18 are potentially cracks occurred in the sample during very early age, potentially due to autogenous shrinkage. Thus, as per the microstructural analysis (SEM) and EDS, ASR gel formation was not detected in any of the alkali activated slag concrete samples despite the higher expansion observed in these samples. In summary, it appears that the excessive expansion is not caused by typical ASR reaction in the system.
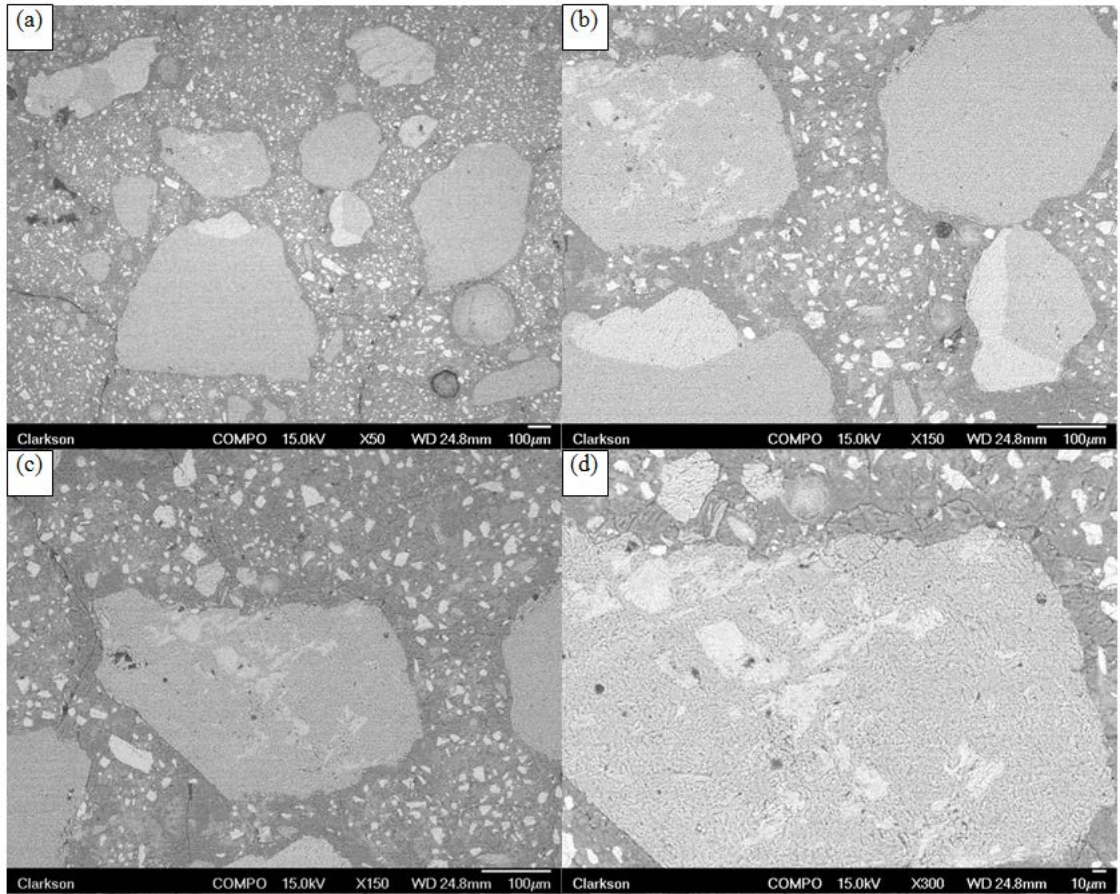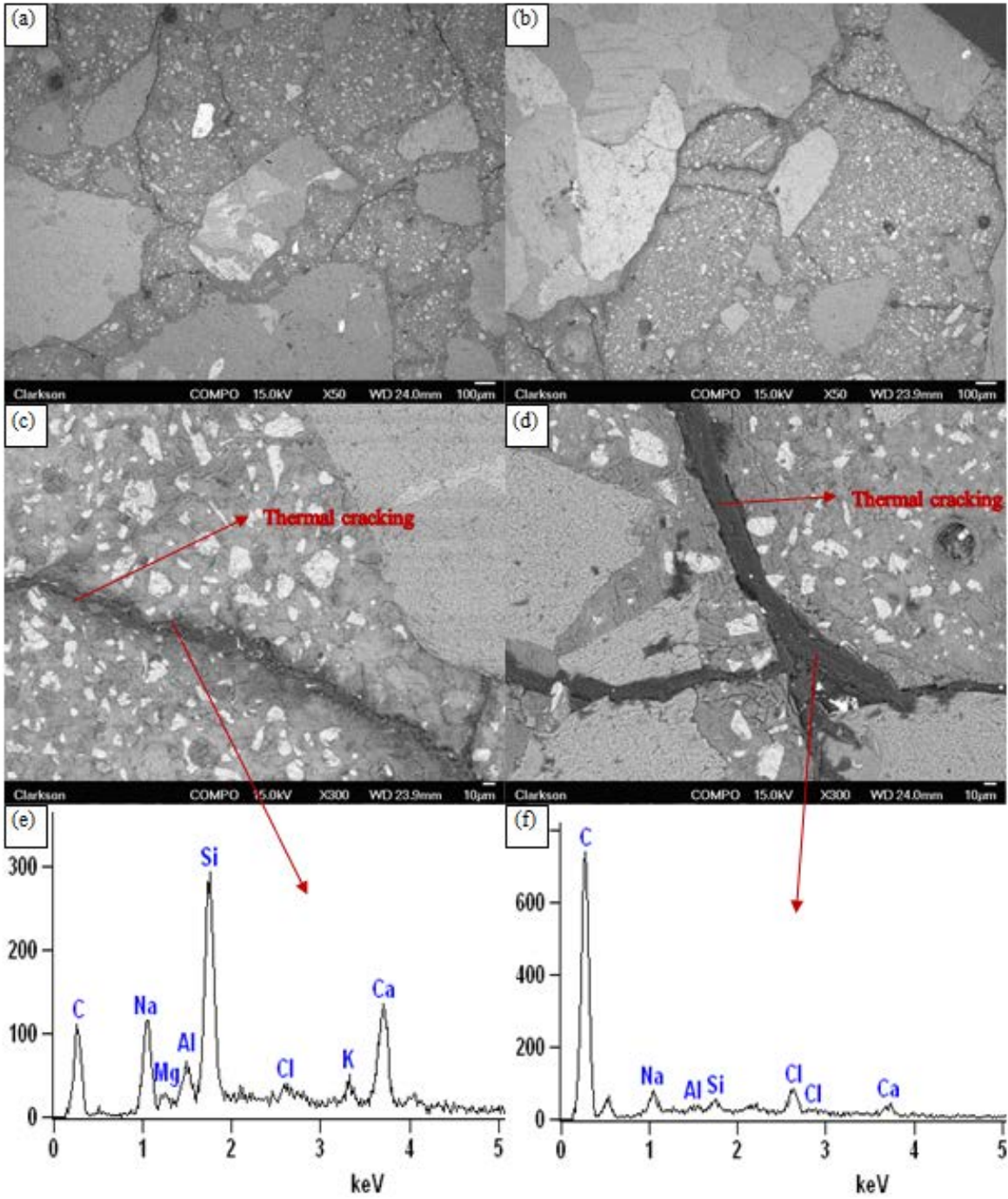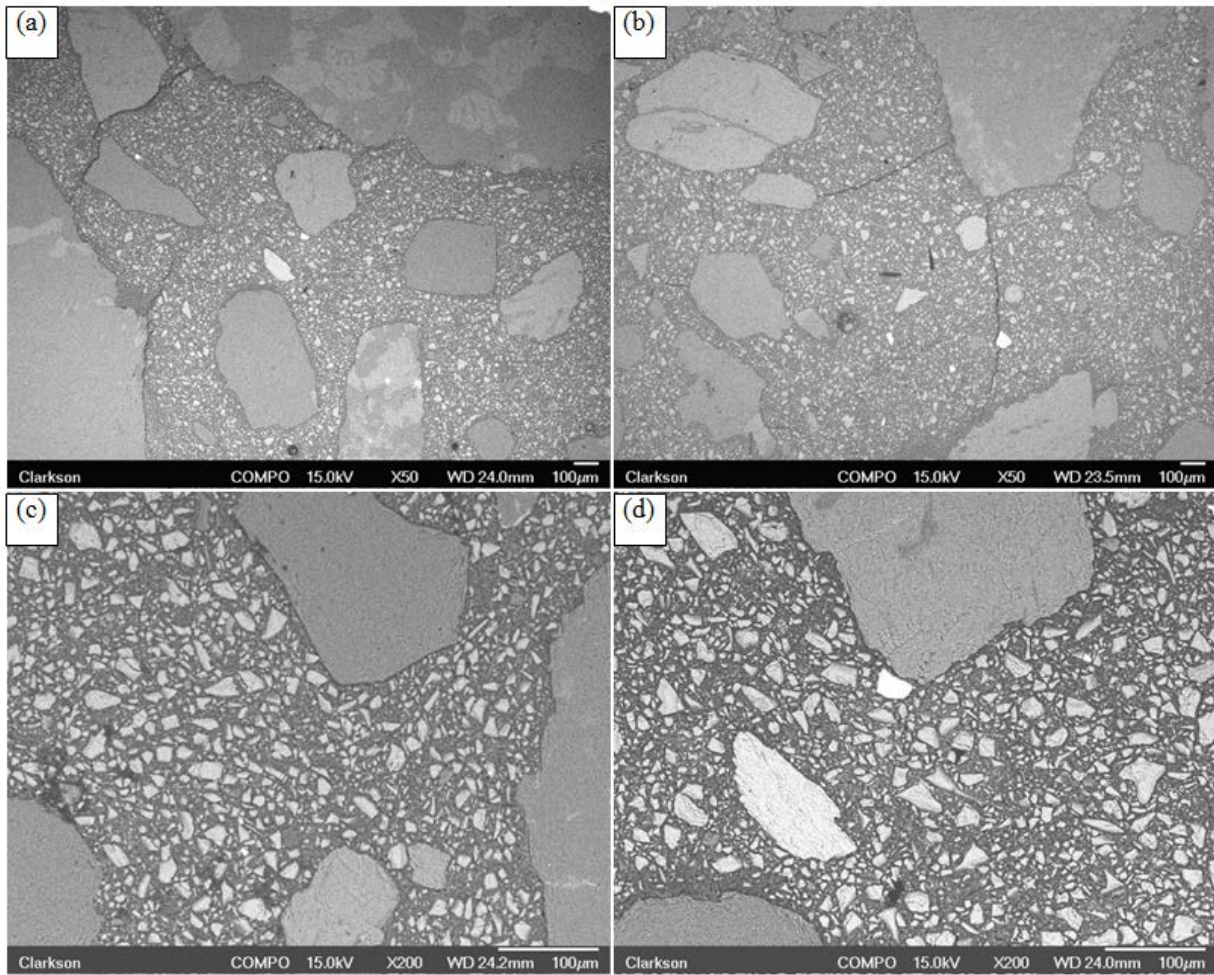
Fig.19 Scanning electron microscopy (Backscattered mode) examination of sodium silicate activated slag concrete with none-reactive aggregate (S2) under test method of ASTM C1293 after 1 year.

Fig.20 Scanning electron microscopy (Backscattered mode) examination and Energy-dispersive X-ray spectroscopy (EDS) of sodium silicate activated slag concrete with none-reactive aggregate (S3) under test method of ASTM C1293 after 1 year

Fig.21 Scanning electron microscopy (Backscattered mode) examination and Energy-dispersive X-ray spectroscopy (EDS) of sodium silicate activated slag concrete with none-reactive aggregate (S4) under test method of ASTM C1293 after 1 year
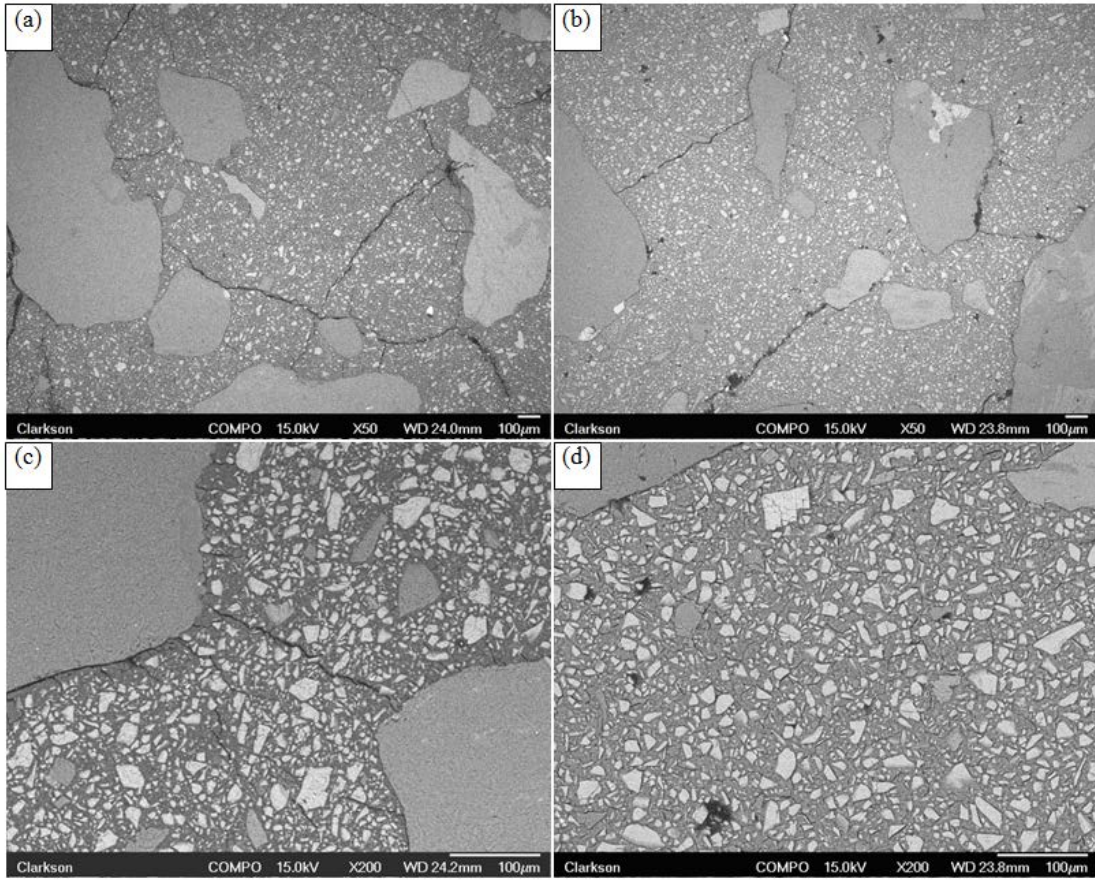
Fig.22 Scanning electron microscopy (Backscattered mode) examination and Energy-dispersive X-ray spectroscopy (EDS) of sodium silicate activated slag concrete with none-reactive aggregate (S5) under test method of ASTM C1293 after 1 year
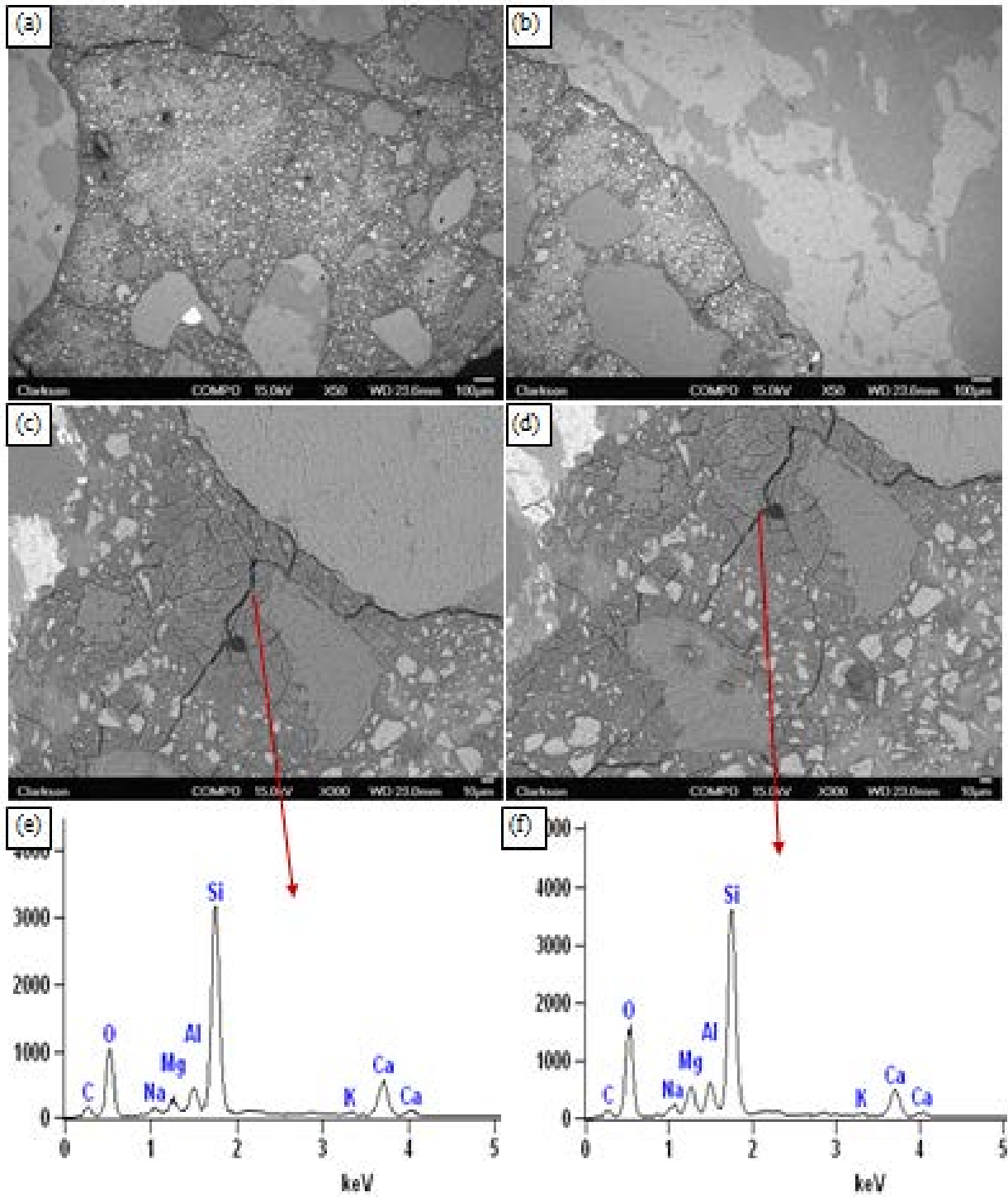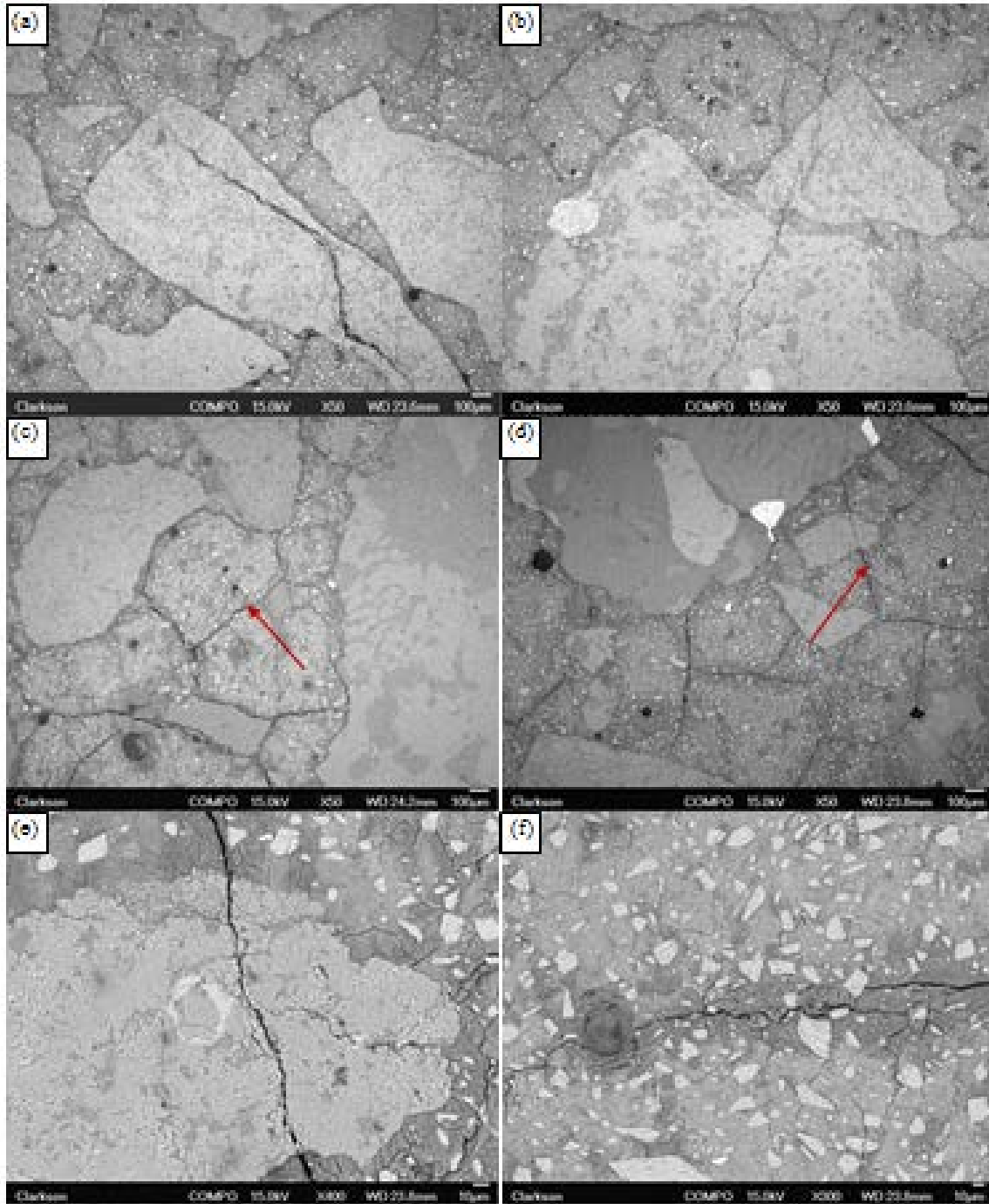
Fig.23 Scanning electron microscopy (Backscattered mode) examination and energy-dispersive X-ray spectroscopy (EDS) of sodium hydroxide activated slag concrete with none-reactive aggregate (S7) under test method of ASTM C1293 after 1 year

3.2.3 Alkali Activated Slag with Reactive Aggregate

Alkali activated slag concrete with reactive aggregate (Spratt aggregate) was examined under BSEM and images with different magnifications are presented in Fig. 24. As shown in the figure abundant notable cracks across aggregates and in hardened cement paste matrix areas was identified from AASC with reactive aggregate (S2-Rx). One may also observe from Fig. 24 (c and d) that polygonal shaped cracks or map-cracking also formed in the cement paste matrix area around the reactive aggregate. Although, numerous cracks in the aggregate as well as the paste area were found, unlike in OPC concrete with reactive aggregates (Fig. 18 (d)), most of those cracks were empty and not much gel was found inside these cracks.

Additional examination using fractured samples under secondary mode was conducted to further analyze the ASR gel in samples containing reactive aggregate (S2-Rx). Secondary mode micrographs of mixture S2-Rx at various magnifications are shown in Fig.25 and Fig.26, and representative EDS spot points showing the composition within that microstructure. The low-magnification image in Fig.25-a and Fig.26-a indicates abundant microcracking near the aggregate-paste matrix interface. Additionally, the higher-magnification images in Fig.25 (c and d) and Fig.26 (c and d) indicate the formation of a rosette-shaped crystalline product within those cracks, which is likely to be ASR gel. The EDS spectrum of that crystalline product (Fig.25-f and Fig.26-f) contains mainly silicon (Si), sodium (Na), and calcium (Ca), which is very similar to the composition of the ASR gel formed in portland cement concrete with reactive aggregate (OPC-Rx). It is evident that the SEM images of AAS are consistent with expansion and mass change results in Fig.2, in which the content of the S2-Rx expanded dramatically compares to S2.

Fig.24 Scanning electron microscopy (Backscattered mode) examination of alkali activated slag concrete with reactive aggregate (S2-Rx) under test method of ASTM C1293 after 1 year
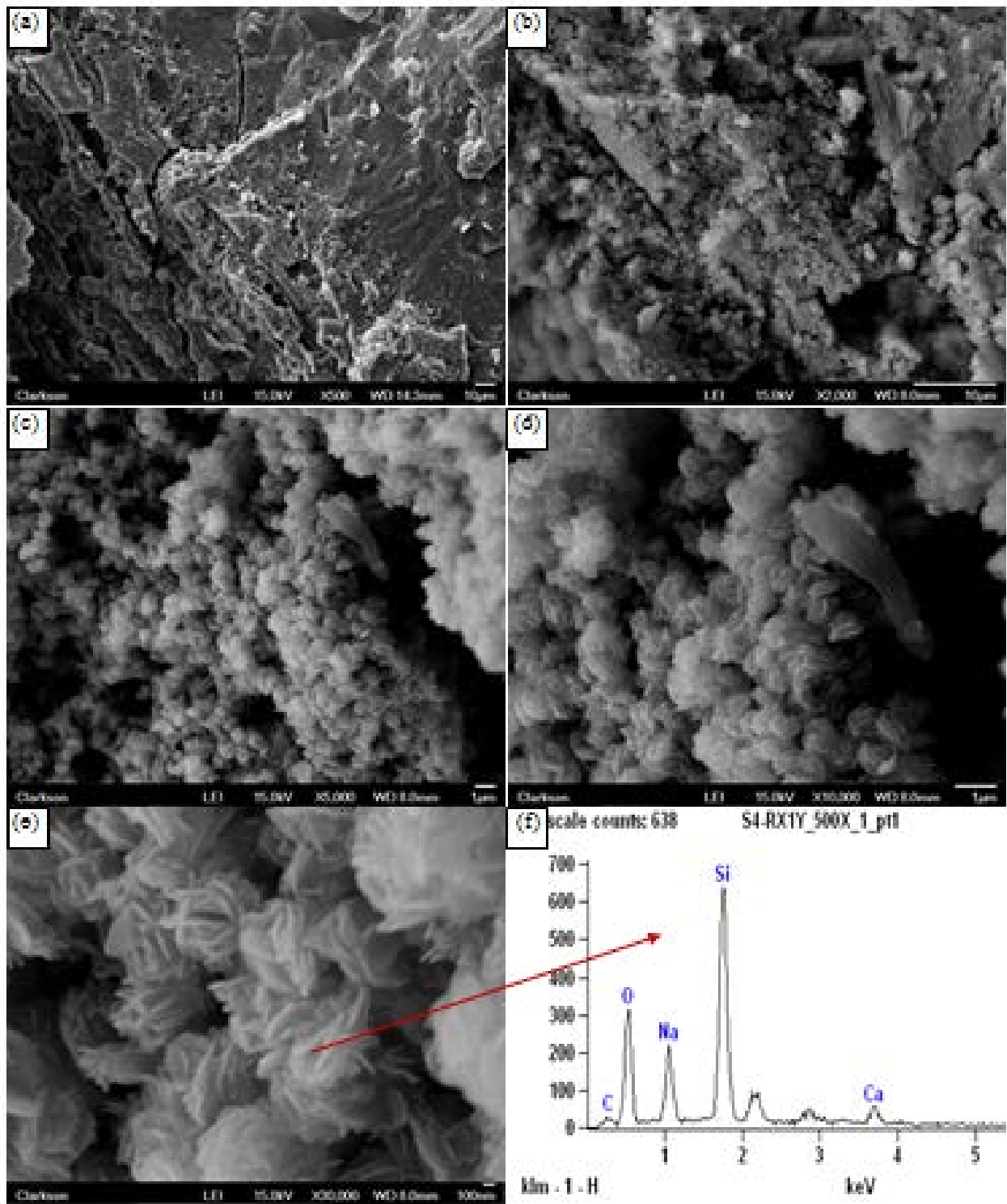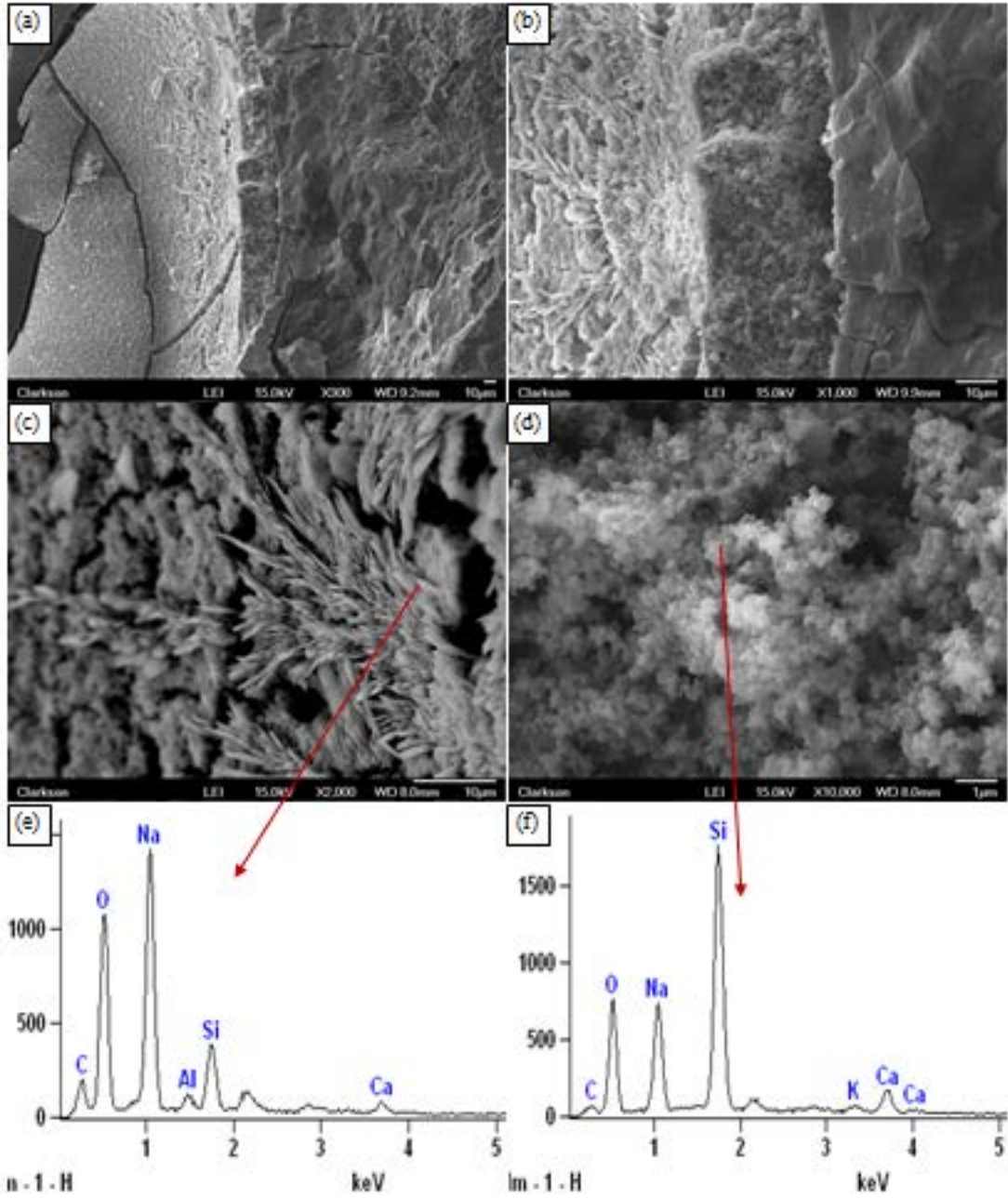
Fig.25 Morphology and chemical composition of reaction product in AASC concrete (S2-Rx) after 1-year exposure to ASTM C1293 test condition

Fig.26 Morphology and chemical composition of reaction product in AASC concrete (S2-Rx) after 1-year exposure to ASTM C1293 test conditions

3.2.4 Potential Alkali Carbonates Reaction

Since some of the alkali activated slag concrete samples containing non-reactive aggregates (S2, S3, S4, S5 and S7) expanded beyond the stipulated limit by ASTM 1293 and no ASR gel was found in those concrete using SEM/EDS, further analyses were conducted to discount potential alkali carbonate reaction (ACR) in these systems. To verify the limestone coarse aggregate used in the AAC, normally known to be a non-reactive in OPC concrete, did not cause any alkali carbonate reaction,   further microscopic analysis were conducted. The SEM-EDS was used to examine coarse aggregate and the surrounded areas to verify the uncertainty of alkali carbonate reaction occurred in AASC. Representative images and EDS spectra are displayed in Fig.27. The examination did not find (1) micro cracking within the coarse aggregate, (2) deposition of magnesium hydroxide, which is known as the main ACR product, (2) inclusion of clays around a local magnesium carbonate deposit in the aggregate, and hence the presence of ACR was discounted as the reason for the expansion of AAC samples. Thus, as discussed in Fig.6,a dramatic drop in the internal humidity and the consequent moisture absorption when subjected to 100 % RH during the ASTM C 1293 exposure conditions could be the reason for the observed expansion in some of these alkali activated slag concrete mixtures.
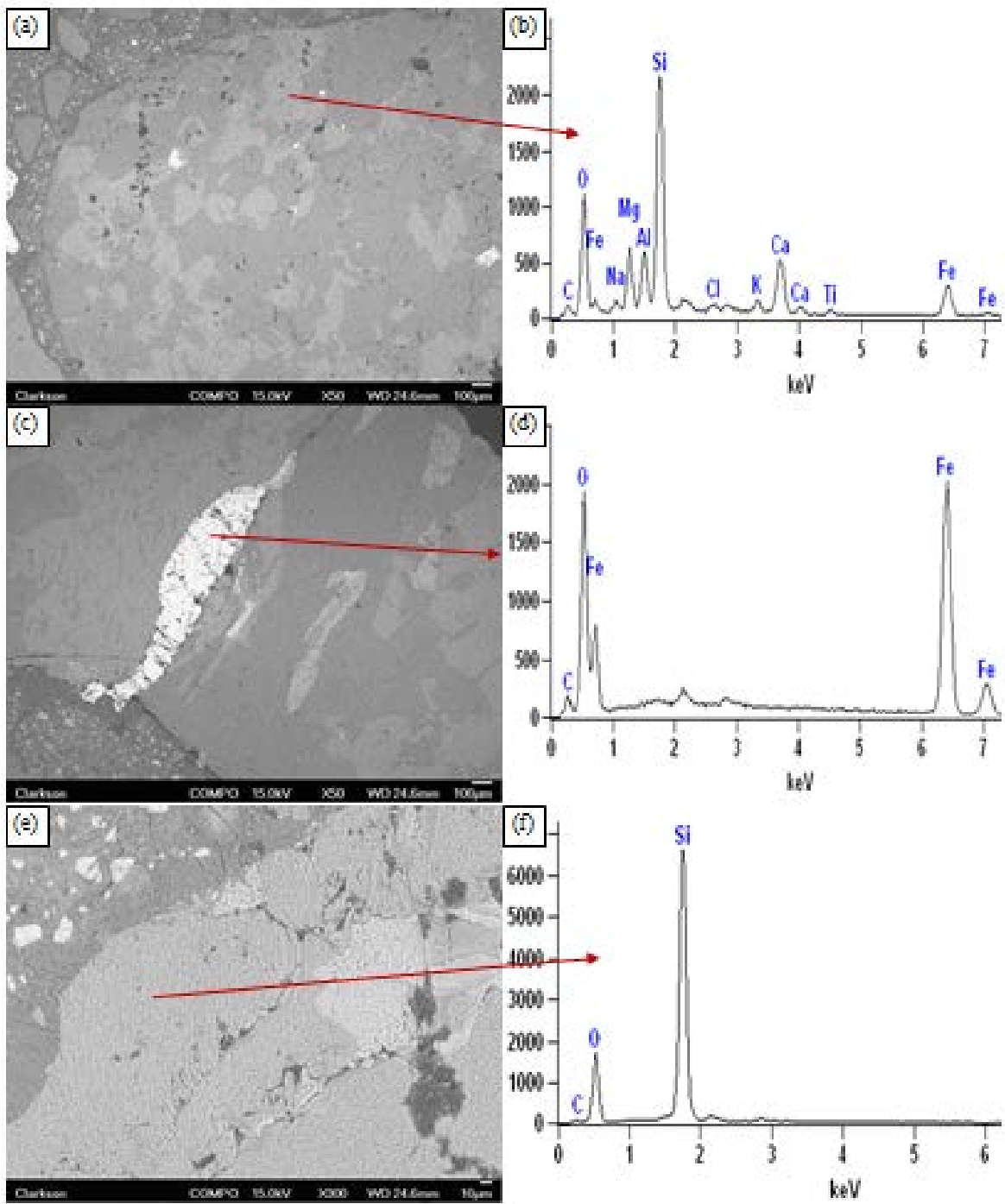
Fig.27 Scanning electron microscopy (Backscattered mode) examination of coarse aggregate in alkali activated slag concrete (S2) under test method of ASTM C1293 after 1 year

3.2.5 Alkali Activated Class C Fly Ash Concrete

Figs.28 and 29 show the backscatter mode scanning electron micrograph (BSEM) images of alkali activated fly ash concrete with none reactive aggregate after 1-year exposure under ASTM C1293. The pair of images show representative areas of the polished specimens at varies magnifications (50× to 300×) to give different views of microstructure after samples exposed to long-term ASR test. Here, one may observe the well-established microstructure of hardened alkali activated binder with unreacted fly ash particles embedded in an apparently continuous gel matrix connecting the unreacted portions of the starting material grains together. Several micro cracks were found in the paste regions but none in the aggregate. It was found in other studies that alkali activated class C fly ash are prone to more micro cracking even during the curing period. Further EDS analysis of areas in and around the cracks did not identify any ASR gels. Thus, ASR reaction was not occurring in alkali activated class C fly ash concrete while non-reactive aggregate was used. It should be recalled that none of the fly ash containing alkali activated concrete experienced any expansion. The measured expansion after one-year exposure period was only 200 $\mu\varepsilon$ (Fig.2).

Fig.30 shows the microstructure of the alkali activated fly ash concrete with reactive aggregate Spratt. In general, several micro cracking were generated across the reactive aggregate in FC2-Rx. However, no ASR gel was found in alkali activated fly ash concrete with both aggregate type. Even with the presence of reactive aggregate, the expansion was close to 500 $\mu\varepsilon$ only at the end of one year exposure period. The petrographic results presented here shows a consistency with the expansion, mass change and dynamic modules trends displayed in Fig.2. Furthermore, it is evident that no deleterious ASR occurred in alkali activated fly ash concrete when non-

reactive aggregate was used, and the microcracking across the aggregate is probably the main potential reasons for the excessive expansion in FC2-Rx.

Fig.28 Scanning electron microscopy (Backscattered mode) examination of alkali activated class C fly ash concrete with none-reactive aggregate (FC2) under test method of ASTM C1293 after 1 year

Fig.29 Scanning electron microscopy (Backscattered mode) examination of alkali activated class C fly ash concrete with none-reactive aggregate (FC4-H) under test method of ASTM C1293 after 1 year

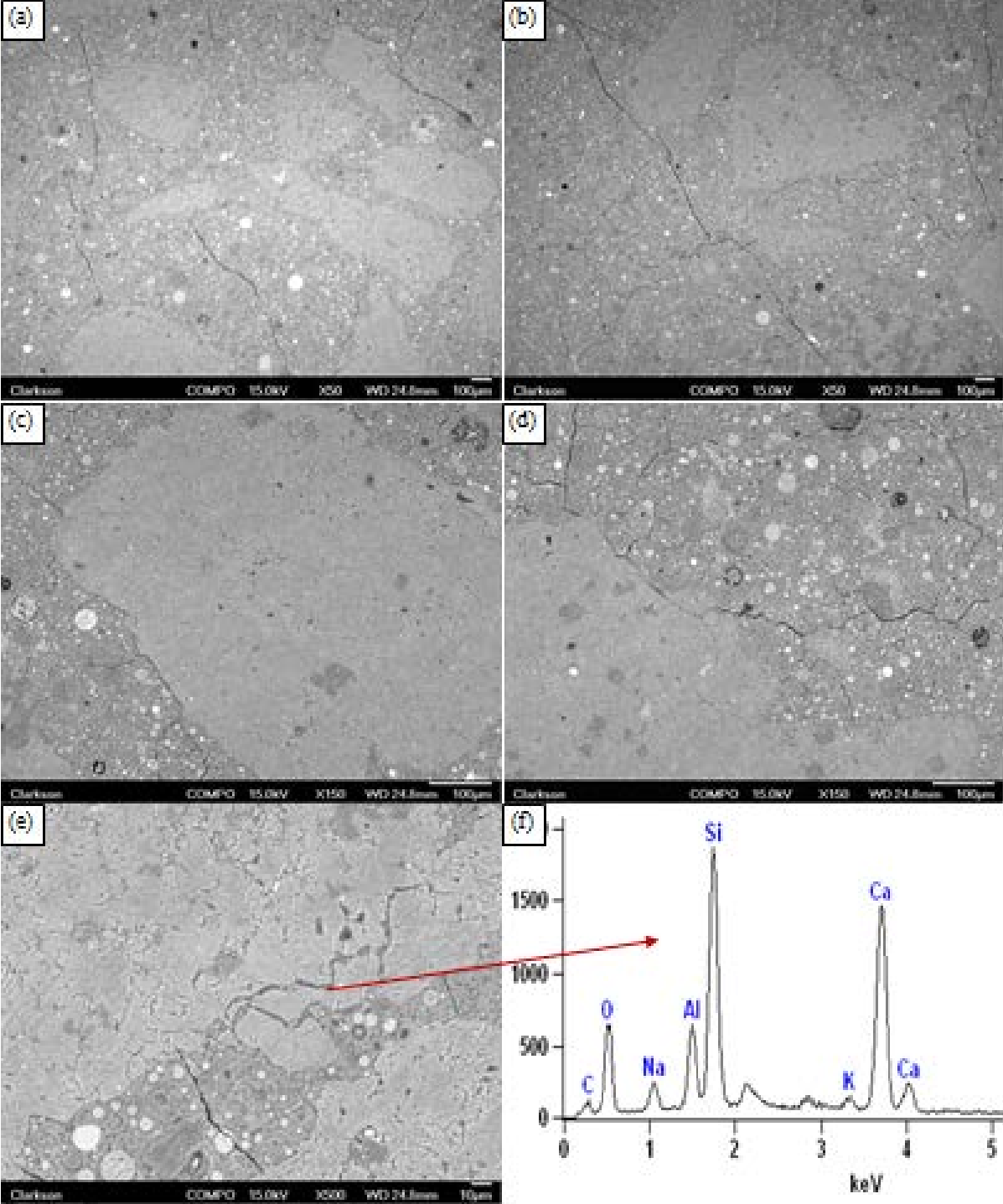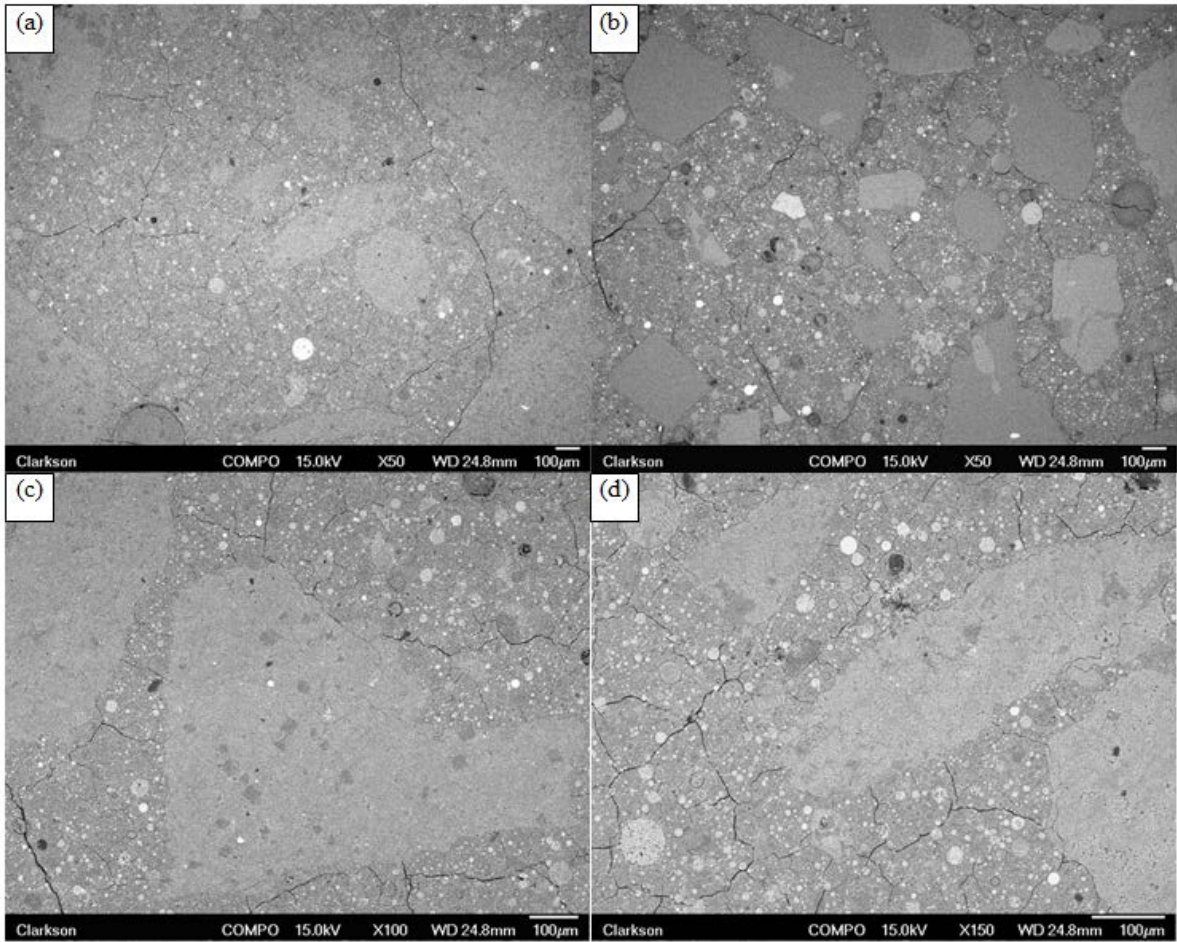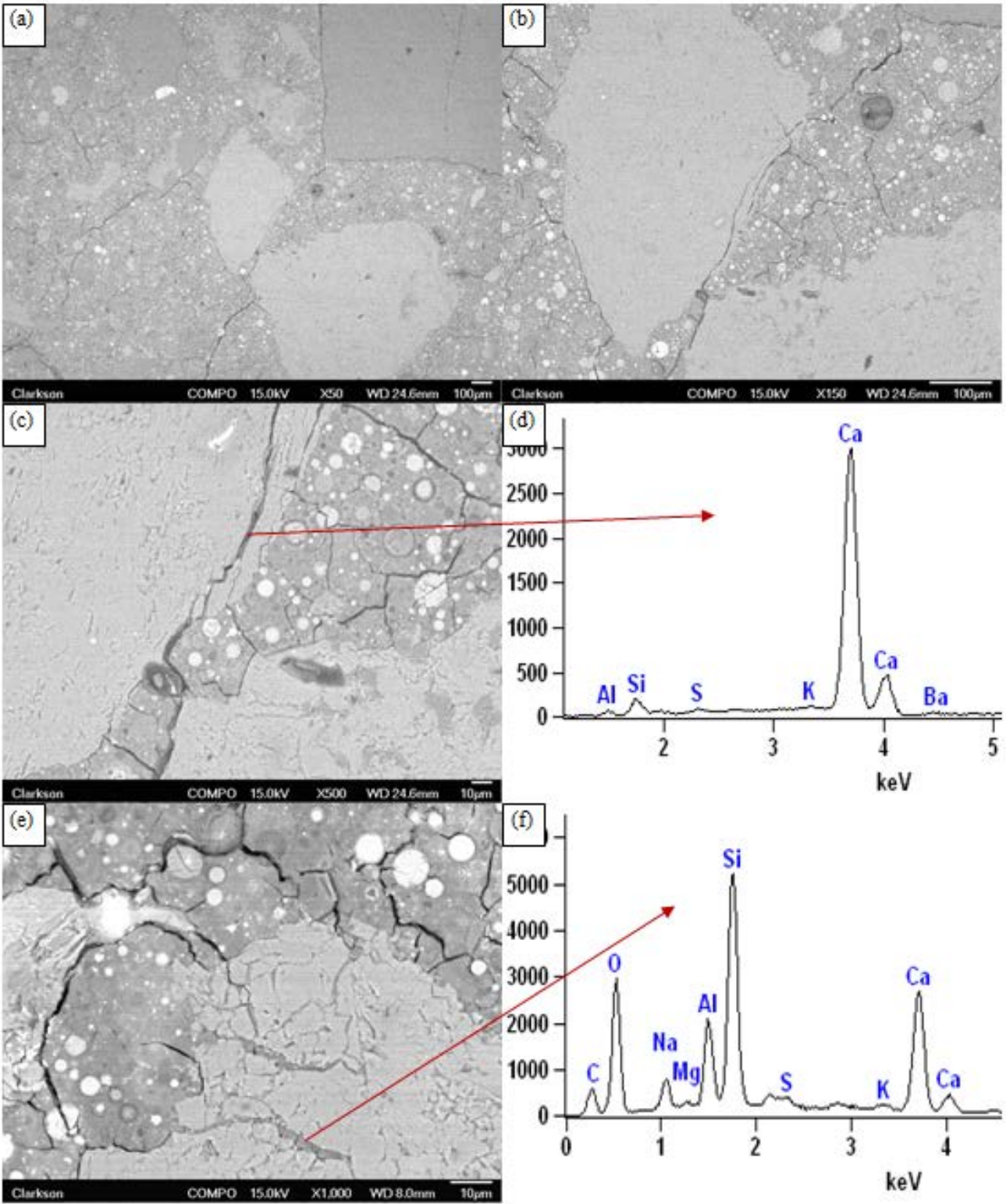**Fig.30 Scanning electron microscopy (Backscattered mode) examination of alkali activated class C fly ash concrete with reactive aggregate (FC2-Rx) under test method of ASTM C1293 after 1 year**

53

3.3 Pore solution Analysis

The objective of the pore solution analysis was to determine composition of the pore solution, especially the amount of sodium and silica in the pore solution. The presence of other ions such as Mg^{+2}, Al^{+3}, and S can also be analyzed. The variation of alkali (Na^+) is most important for evaluating the ASR resistance. The variation in sodium ion is depicted in Fig. 31 (a). As can be seen in this figure, the Na^+ ions in the solution exponentially decreased with hydration time. At the end of eight hours, the concentration of the Na^+ ions dropped from approximately ~2500 mmol/L to 750 mmol/L (70% reduction) in highly concentrated activator system. A similar drop can be noted in the concentration of the dissolved silica. Fig 31 (b) shows the variation of silica in the system. The removal of Si from the system for the formation of new product is evident and follows a trend similar to that of Na^+ ions in the system. This means, most of the Na^+ is bound in the hydration products early on during the hydration period itself. It is also evident that the reduction in the Na^+ ions continues beyond 8 hours in the high Na_2O content mixtures. As the hydration time increases, most of the alkali (Na^+) could be bound the reaction products. Class C fly ash containing mixtures also exhibited a similar trend. The analysis shows the Na^+ will be consumed during the reaction process and only a small amount will be left in the pore solution. This small percentage of Na^+ remaining in the system may not cause ASR gel formation in these concrete especially in the absence of calcium hydroxide. This could be the reason for the absence of ASR in alkali activated concrete containing non-reactive aggregate. Further in depth scientific analysis is needed to explain the absence of ASR gel in the cracks of some of the concrete with reactive aggregate despite showing extensive expansion and cracking.
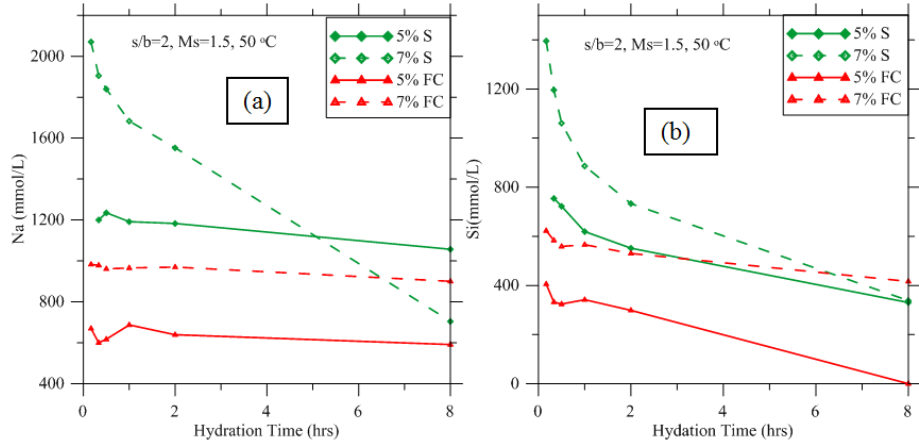
Fig. 31 Pore solution analysis showing the concentration of (a) Na$^+$ and (b) Si$^+$ in AAC systems (s-slag and FC- class C fly ash)

4. Conclusions and recommendations

The alkali-silica reactivity of AAC binders was evaluated under different ASR test methods and by petrography. The DME was used to monitor the physical deterioration of the samples due to ASR. Several important conclusions can be drawn from the results of this investigation.

- Results from this study show that both the long-term ASTM test method C1293 and accelerated C1567 are appropriate for evaluating the potential ASR reactivity of alkali activated systems. Both the test methods had given some false positive test results when there was no ASR occurred in the system. Hence, it is recommended to use petrographic analysis as a supplementary test to verify the findings of ASTM C1293 and C1567 test results. Several alkali activated slag cement concrete samples experienced expansion beyond the stipulated limit of ASTM C1293. Those samples had excessive autogenous shrinkage and very low internal relative humidity before exposing them to the test environment (100% RH, specifically). Samples absorbed moisture immediately after exposing it to the test environment and expanded ~400 $\mu\varepsilon$ even during the first week of exposure to ASTM C 1293 test condition. It is recommended either to precondition the samples (such as heat curing the samples to 40^0C for 24 hours and soaking it in water for another day before exposing the samples to ASTM C1293) or it is required to increase the expansion limit from 400 $\mu\varepsilon$ to 1000 when evaluating slag cement based AAC with excessive autogenous shrinkage and low internal relative humidity.

- The expansion limit seemed more appropriate in the case of AAFC, most of AAFC specimens are within the limit unless reactive aggregates were used in the experiment.

- No deleterious alkali-silica reaction was observed in AASC and AAFC concrete with non-reactive aggregate.

- Significant micro cracking with massive ASR gel were identified within OPC-Rx specimen by Backscattered Scanning Electron Microscopy (BSEM), and it also confirms that the Ottawa Spratt siliceous limestone aggregate used in the study was a reactive aggregate.

- The ASR product, a rosette-shaped crystalline product was observed in AASC with reactive aggregate. The morphology and composition of that product was similar to that typically observed in OPC binders. It should be noted that even in samples with reactive aggregate, the cracks in the aggregates were always empty without any gels unlike in the OPC system. Also, it was hard to find extensive amounts of ASR gels throughout the sample.

- No alkali carbonate reaction (ACR) occurred in the system with the limestone coarse aggregate used in this study.

- The composition and concentration of the activator and curing conditions influences the expansion and mass change in ASR test specimens, but there is no evidence that these parameters affect the alkali-silica reactivity significantly.

- The DME is a good test to monitor the cracking and deterioration of the samples due to ASR. DME values did not change with exposure period in concrete with reactive aggregate, indicating the absence of extensive cracking and deterioration. The test results were consistent with the petrographic analysis. The DME of the specimens with reactive aggregate showed degradation in the values with time.

- The better resistance of AAC to ASR can be attributed to the less availability of free alkali in the AAC system due to the binding of most of the alkali by the reaction products (70% by 8 hours) very early on during hydration and the absence of calcium hydroxide in the AAC system.

Publication and presentation

Peer reviewed conference proceedings:

Li, Z., and S. Peethamparan. ," Evaluation of ASTM Method for Detection of Alkali-Silica Reaction in Alkali-Activated Concrete", The 96th Annual Meeting of the Transportation Research Board, Washington, D.C, US, Jan 10-14, 2017

Presentation:

Li, Z., and S. Peethamparan., "Alkali-Silica Reaction (ASR) Susceptibility of Alkali-Activated Cement Free Binders", ACI Fall Convention 2016, Philadelphia, PA, Oct 23-27,2016

References

1. Worrell, E., L. Price, N. Martin, C. Hendriks, and L. O. Meida. Carbon Dioxide Emissions from the Global Cement Industry 1. *Annual Review of Energy and the Environment*, Vol. 26, No. 1, 2001, pp. 303-329.

2. Mehta, P. K. Reducing the Environmental Impact of Concrete. *Concrete International*, Vol. 23, No. 10, 2001, pp. 61-66.

3. Boden, T. A. *Trends' 93: A Compendium of Data on Global Change.* Carbon Dioxide Information Analysis Center, World Data Center-A for Atmospheric Trace Gases, Environmental Sciences Division, Oak Ridge National Laboratory, 1994.

4. Collins, F., and J. Sanjayan. Workability and Mechanical Properties of Alkali Activated Slag Concrete. *Cement and Concrete Research*, Vol. 29, No. 3, 1999, pp. 455-458.

5. Gong, C., and N. Yang. Effect of Phosphate on the Hydration of Alkali-Activated Red Mud–slag Cementitious Material. *Cement and Concrete Research*, Vol. 30, No. 7, 2000, pp. 1013-1016.

6. Bakharev, T., J. Sanjayan, and Y. Cheng. Resistance of Alkali-Activated Slag Concrete to Acid Attack. *Cement and Concrete Research*, Vol. 33, No. 10, 2003, pp. 1607-1611.

7. Fernández-Jiménez, A., I. Garcia-Lodeiro, and A. Palomo. Durability of Alkali-Activated Fly Ash Cementitious Materials. *Journal of Materials Science*, Vol. 42, No. 9, 2007, pp. 3055-3065.

8. Donatello, S., A. Palomo, and A. Fernández-Jiménez. Durability of very High Volume Fly Ash Cement Pastes and Mortars in Aggressive Solutions. *Cement and Concrete Composites*, Vol. 38, 2013, pp. 12-20.

9. McLellan, B. C., R. P. Williams, J. Lay, A. Van Riessen, and G. D. Corder. Costs and Carbon Emissions for Geopolymer Pastes in Comparison to Ordinary Portland Cement. *Journal of Cleaner Production*, Vol. 19, No. 9, 2011, pp. 1080-1090.

10. Duxson, P., J. L. Provis, G. C. Lukey, and J. S. Van Deventer. The Role of Inorganic Polymer Technology in the Development of 'green Concrete'. *Cement and Concrete Research*, Vol. 37, No. 12, 2007, pp. 1590-1597.

11. Douglas, E., A. Bilodeau, J. Brandstetr, and V. Malhotra. Alkali Activated Ground Granulated Blast-Furnace Slag Concrete: Preliminary Investigation. *Cement and Concrete Research*, Vol. 21, No. 1, 1991, pp. 101-108.

12. Shi, C., D. Roy, and P. Krivenko. *Alkali-Activated Cements and Concretes.* CRC press, 2006.

13. Deir, E., B. S. Gebregziabiher, and S. Peethamparan. Influence of Starting Material on the Early Age Hydration Kinetics, Microstructure and Composition of Binding Gel in Alkali Activated Binder Systems. *Cement and Concrete Composites*, Vol. 48, 2014, pp. 108-117.

14. Li, Z., and S. Peethamparan. Influence of Nanosilica and Clay on the Strength, Workability, and Porosity of Alkali-Activated Slag Mortars. In *Transportation Research Board 95th Annual Meeting*, 2016.

15. Diamond, S. ASR-another Look at Mechanisms. In *Proceedings of the 8th International Conference on Alkali-Aggregate Reaction, Kyoto, Japan*, 1989, pp. 83-94.

16. Thomas, M. D., B. Fournier, and K. J. Folliard. *Alkali-Aggregate Reactivity (AAR) Facts Book*, 2013.

17. Swamy, R. N. *The Alkali-Silica Reaction in Concrete.* CRC Press, 2002.

18. Jones, A., and L. Clark. The Effects of ASR on the Properties of Concrete and the Implications for Assessment. *Engineering Structures*, Vol. 20, No. 9, 1998, pp. 785-791.

19. Davidovits, J. Geopolymers. *Journal of Thermal Analysis*, Vol. 37, No. 8, 1991, pp. 1633-1656.

20. Fernández-Jiménez, A., and F. Puertas. The Alkali–silica Reaction in Alkali-Activated Granulated Slag Mortars with Reactive Aggregate. *Cement and Concrete Research*, Vol. 32, No. 7, 2002, pp. 1019-1024.

21. Puertas, F., M. Palacios, A. Gil-Maroto, and T. Vázquez. Alkali-Aggregate Behaviour of Alkali-Activated Slag Mortars: Effect of Aggregate Type. *Cement and Concrete Composites*, Vol. 31, No. 5, 2009, pp. 277-284.

22. Gifford, P., and J. Gillott. Alkali-Silica Reaction (ASR) and Alkali-Carbonate Reaction (ACR) in Activated Blast Furnace Slag Cement (ABFSC) Concrete. *Cement and Concrete Research*, Vol. 26, No. 1, 1996, pp. 21-26.

23. Wang, S., K. L. Scrivener, and P. L. Pratt. Factors Affecting the Strength of Alkali-Activated Slag. *Cement and Concrete Research*, Vol. 24, No. 6, 1994, pp. 1033-1043.

24. García-Lodeiro, I., A. Palomo, and A. Fernández-Jiménez. Alkali–aggregate Reaction in Activated Fly Ash Systems. *Cement and Concrete Research*, Vol. 37, No. 2, 2007, pp. 175-183.

25. Bakharev, T., J. Sanjayan, and Y. Cheng. Resistance of Alkali-Activated Slag Concrete to Alkali–aggregate Reaction. *Cement and Concrete Research*, Vol. 31, No. 2, 2001, pp. 331-334.

26. Puertas, F., M. Palacios, A. Gil-Maroto, and T. Vázquez. Alkali-Aggregate Behaviour of Alkali-Activated Slag Mortars: Effect of Aggregate Type. *Cement and Concrete Composites*, Vol. 31, No. 5, 2009, pp. 277-284.

27. Bakharev, T., J. Sanjayan, and Y. Cheng. Resistance of Alkali-Activated Slag Concrete to Acid Attack. *Cement and Concrete Research*, Vol. 33, No. 10, 2003, pp. 1607-1611.

28. Gebregziabiher, B. S., R. Thomas, and S. Peethamparan. Very Early-Age Reaction Kinetics and Microstructural Development in Alkali-Activated Slag. *Cement and Concrete Composites*, Vol. 55, 2015, pp. 91-102.

29. Deir, E., B. S. Gebregziabiher, and S. Peethamparan. Influence of Starting Material on the Early Age Hydration Kinetics, Microstructure and Composition of Binding Gel in Alkali Activated Binder Systems. *Cement and Concrete Composites*, Vol. 48, 2014, pp. 108-117.

30. Jawed, I., J. Skalny, and J. Young. Hydration of Portland Cement. *Structure and Performance of Cements.Essex: Applied Science Publishers*, 1983, pp. 284-285.

University Transportation Research Center - Region 2

Funded by the U.S. Department of Transportation

Region 2 - University Transportation
Research Center
The City College of New York
Marshak Hall, Suite 910
160 Convent Avenue
New York, NY 10031
Tel: (212) 650-8050
Fax: (212) 650-8374
Website: www.utrc2.org